Inferring the variation in redshift of the binary black hole merger rate combining gravitational-wave searches

Max Lalleman*[1] , Kevin Turbang[1,2], Thomas A. Callister[3], Nick van Remortel[1]

1 Universiteit Antwerpen, B-2000 Antwerpen, Belgium

2 Theoretische Natuurkunde, Vrije Universiteit Brussel, B-1050 Brussel, Belgium

3 University of Chicago, Chicago, Illinois, USA

* max.lalleman@uantwerpen.be

Gravitational waves

Gravitational waves (GWs) are a consequence of General Relativity.
They exist in multiple forms:

- **Chirps from massive object mergers**
- Bursts
- Continuous waves (see talk Luca)
- **Stochastic gravitational-wave background (SGWB)**

In our analysis, we focus on chirps and the results from the search for the SGWB.

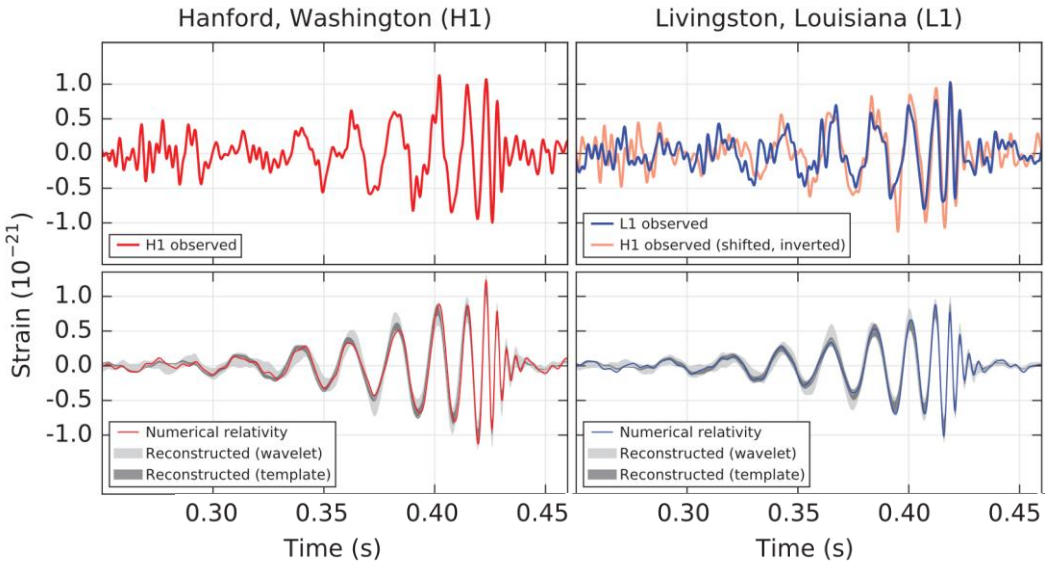

Fig. 1: Example of a chirp event, specifically the first one ever observed GW150914.
Phys. Rev. Lett. 116, 061102

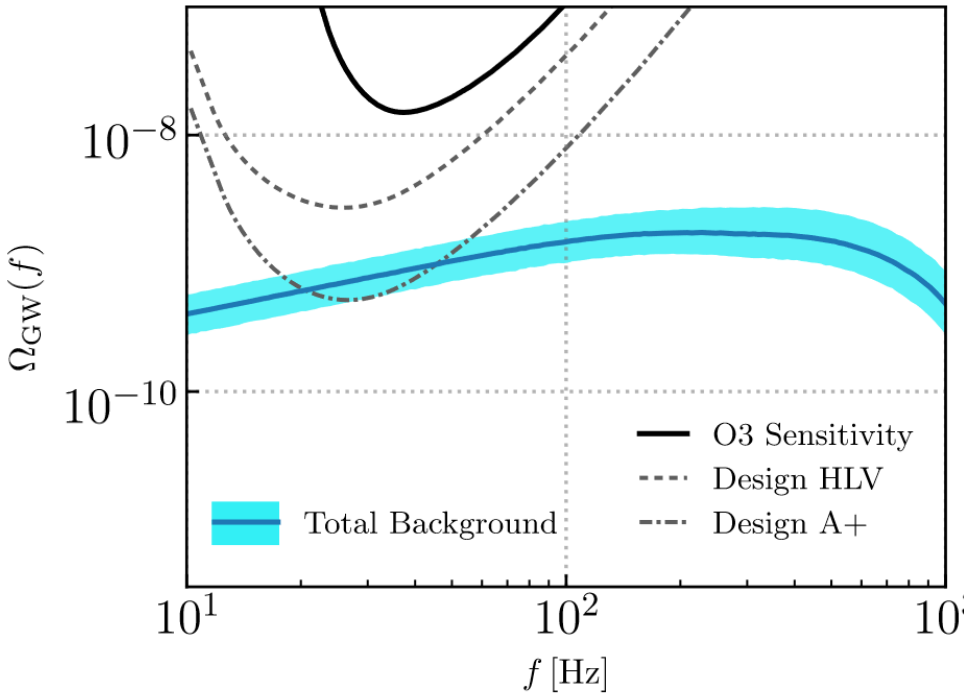

Fig. 2: The computed SGWB based on the chirps coming from alle events discovered in the previous observing runs of the LIGO-Virgo-KAGRA (LVK) collaboration. Phys. Rev. X 13, 011048

Network of detectors

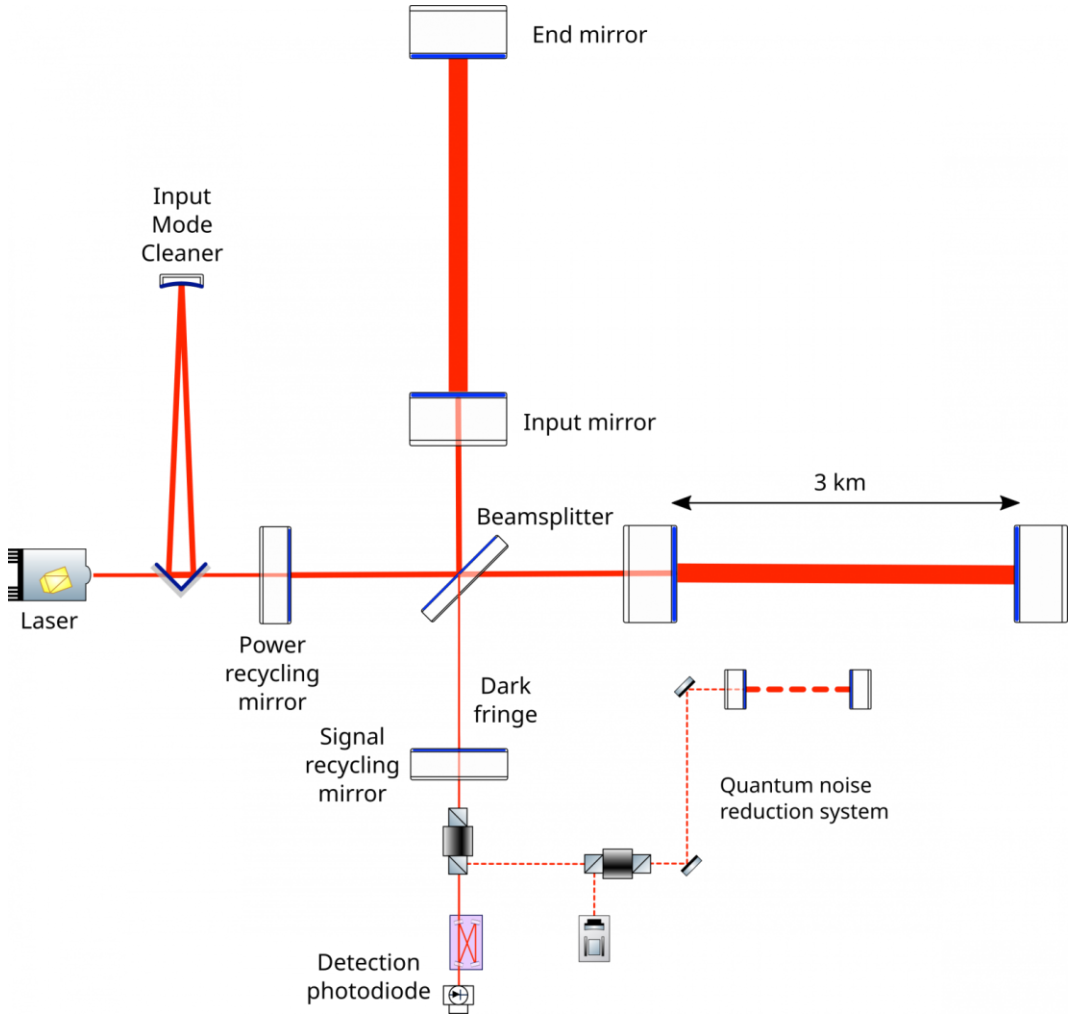

Fig. 3: The optical layout of Advanced Virgo. https://www.virgo-gw.eu/science/detector/optical-layout/

Global network of interferometers searching for GWs.
Laser destructive interference searching for signals.

Future: LISA, Einstein Telescope, Cosmic Explorer

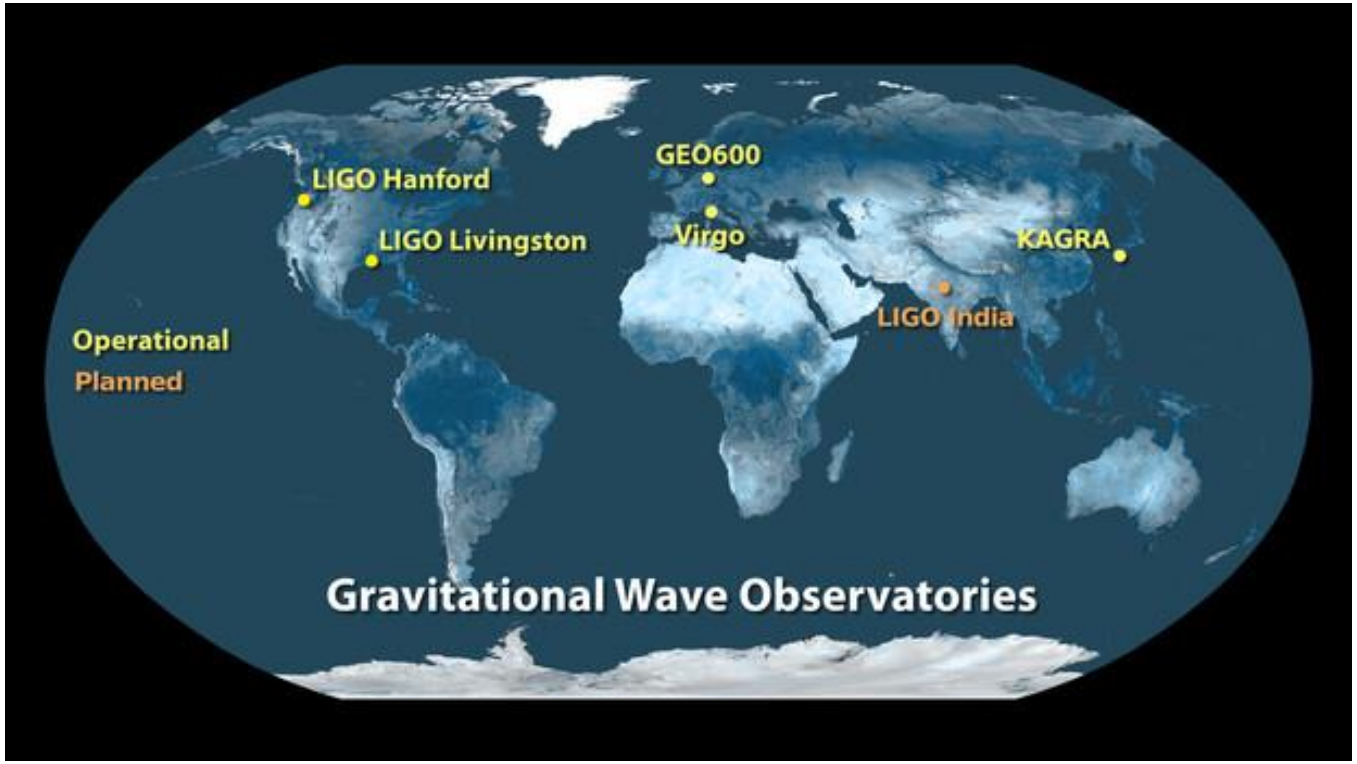

Fig. 4: The global network with all current interferometers, not next generation. https://www.ligo.caltech.edu/image/ligo20160211c

Chirps

Chirps are transient signals of massive object mergers.
Main channels for chirps are:

- **Binary black hole (BBH) mergers**
- Binary neutron star (BNS) mergers
- Neutron star - black hole (NSBH) mergers

Most detected chirps are from BBH mergers.
These have higher masses than EM-observed objects.

Chirps are observed at low to moderate redshift.

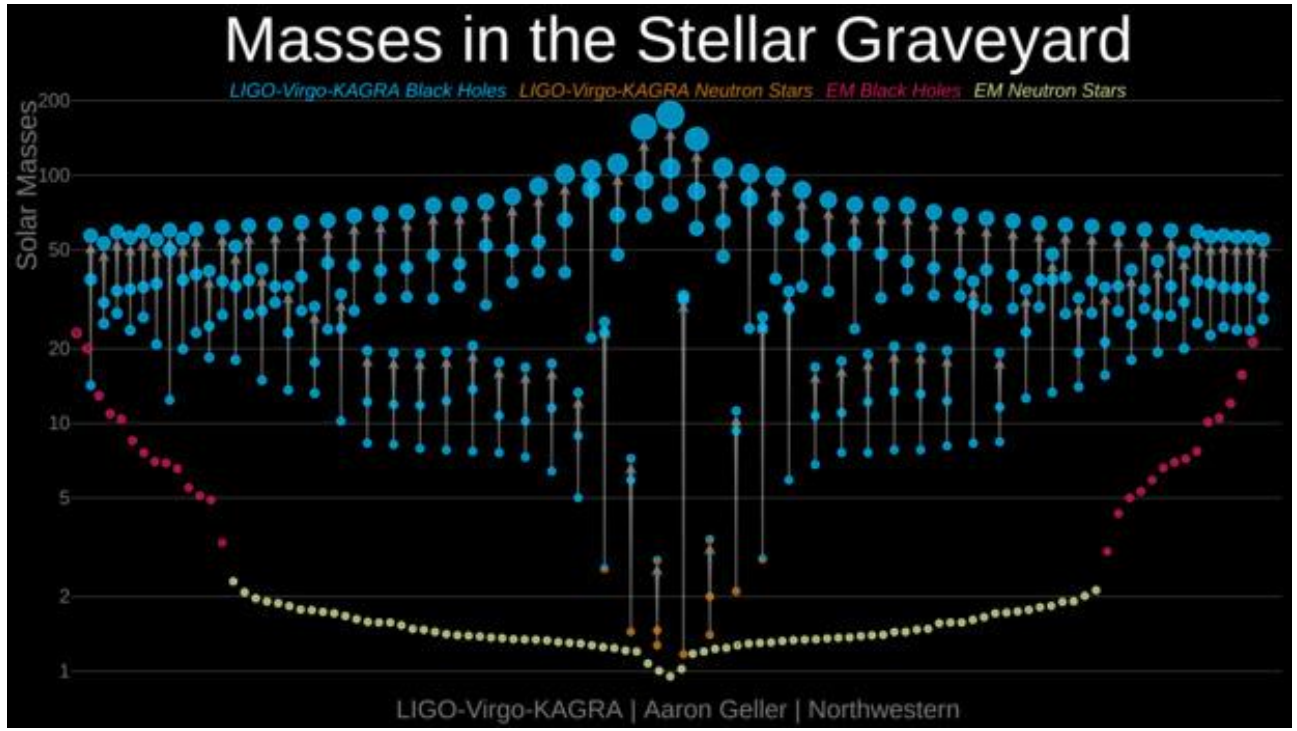

Fig. 5: This graphic shows all the masses for all GW events so far observed in LVK. https://www.ligo.caltech.edu/LA/image/ligo20211107a

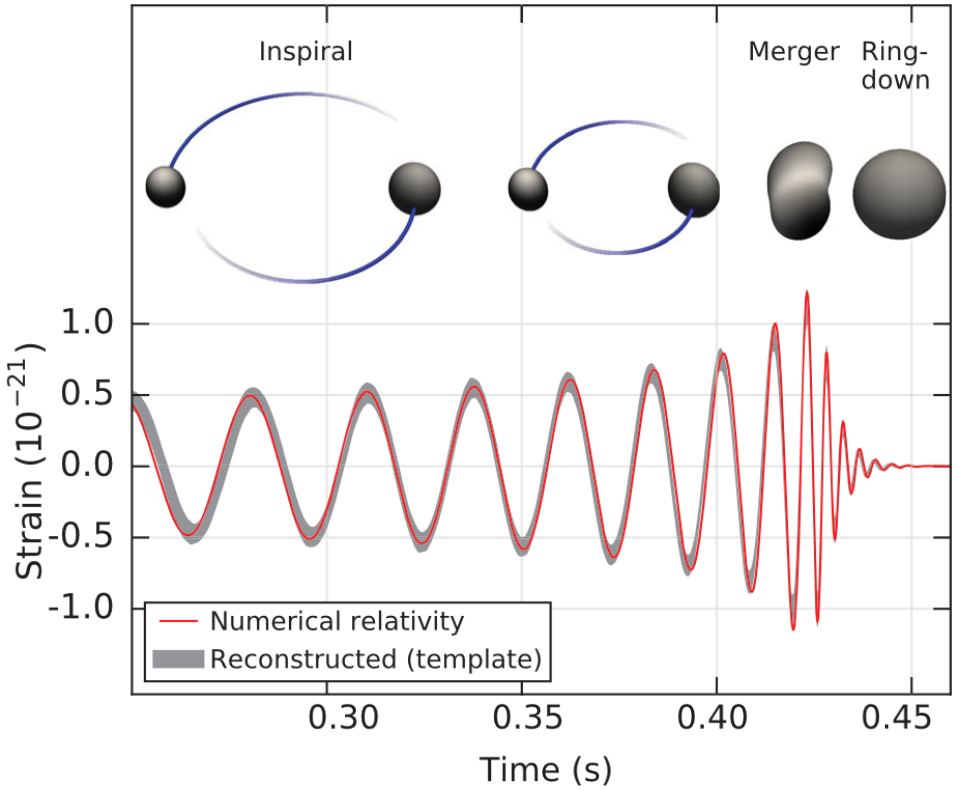

Fig. 6: Example of reconstructing the first ever chirp GW150914. Phys. Rev. Lett. 116, 061102

Stochastic gravitational-wave background

The SGWB is a superposition of weak GW sources.
It can exist in many forms from two categories:

- **Astrophysical background**
- Cosmological background

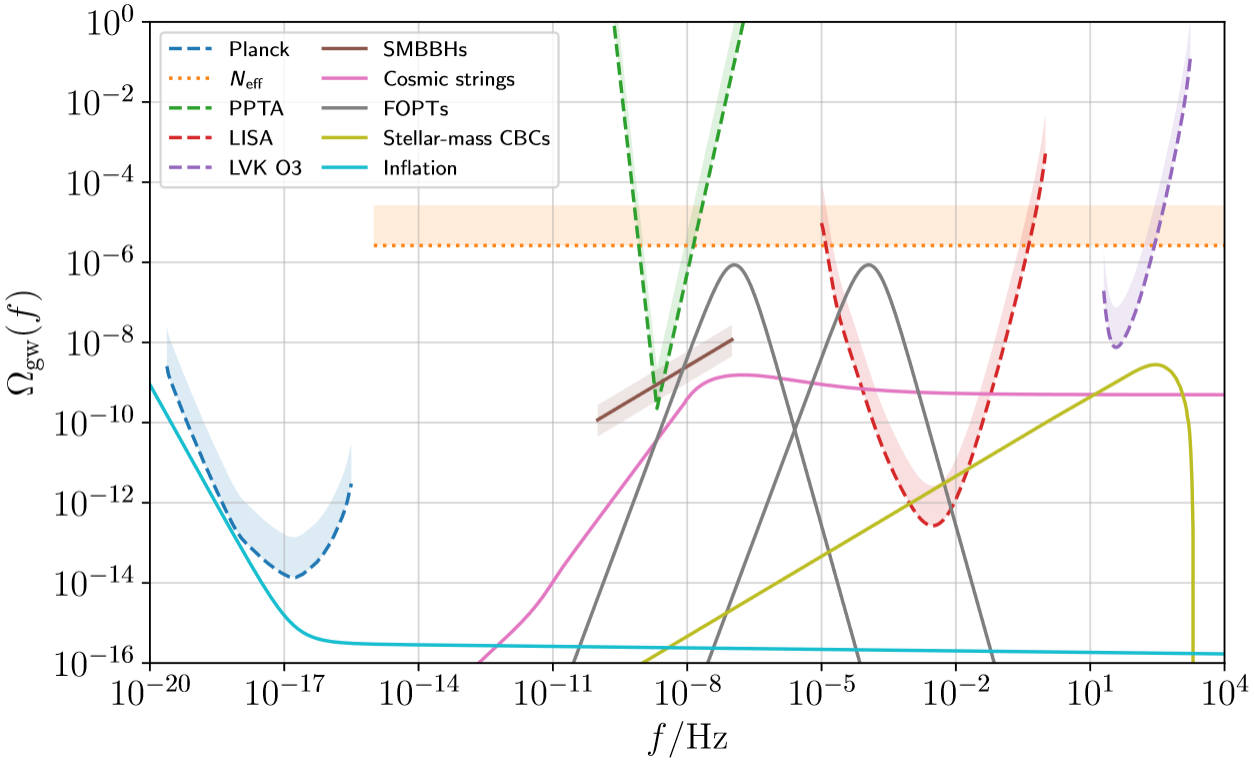

Fig. 7: Overview of potential background signals across the frequency spectrum. Showing both sensitivity curves from experiments as dotted lines and expected background magnitudes as solid lines. Galaxies 2022, 10(1), 34

Stochastic gravitational-wave background

The SGWB is a superposition of weak GW sources.
It can exist in many forms from two categories:

- **Astrophysical background**
- Cosmological background

- **(Un)resolvable chirps**
- Core collapse supernovae
- Rotating neutron stars

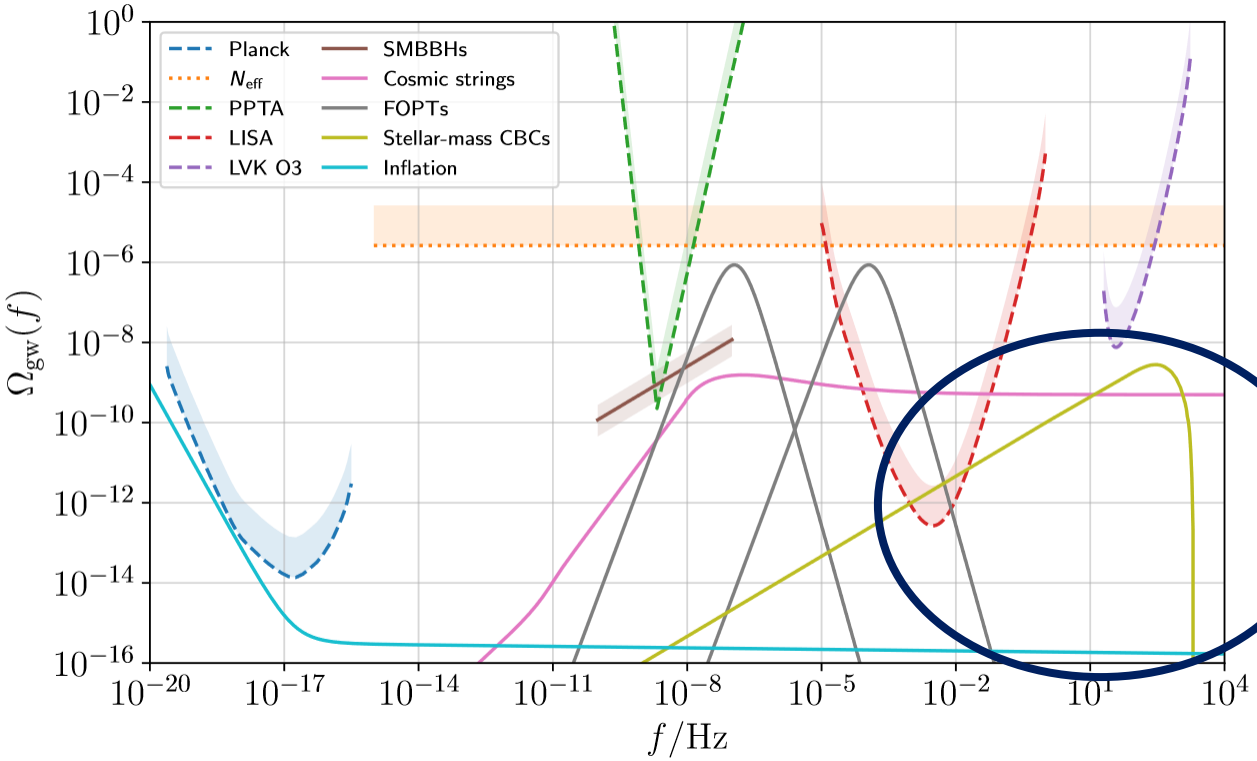

Fig. 7: Overview of potential background signals across the frequency spectrum. Showing both sensitivity curves from experiments as dotted lines and expected background magnitudes as solid lines. Galaxies 2022, 10(1), 34

Stochastic gravitational-wave background

The SGWB is a superposition of weak GW sources.
It can exist in many forms from two categories:

- **Astrophysical background**
- Cosmological background

- **(Un)resolvable chirps**
- Core collapse supernovae
- Rotating neutron stars

- Primordial black holes
- Cosmic strings
- Inflation
- Phase transitions
- …

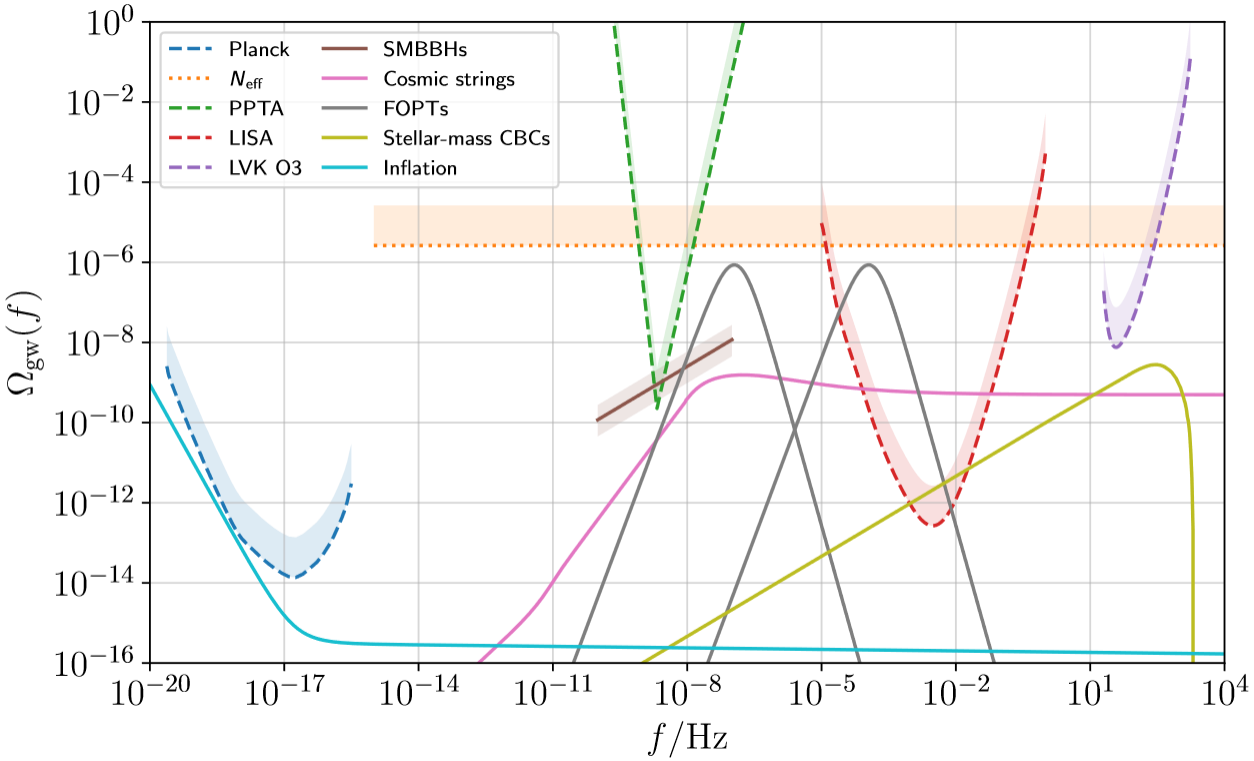

Fig. 7: Overview of potential background signals across the frequency spectrum. Showing both sensitivity curves from experiments as dotted lines and expected background magnitudes as solid lines. Galaxies 2022, 10(1), 34

The SGWB is characterized by energy density

$$\Omega_{\rm GW}(f) = \frac{1}{\rho_c}\frac{d\rho_{\rm GW}(f)}{d\ln f}$$

Since we are only interested in BBH events, we only look at the astrophysical background from BBHs.

Astrophysical background

The astrophysical background can be estimated from all observed events.

We estimate that we would observe the background at design A+.

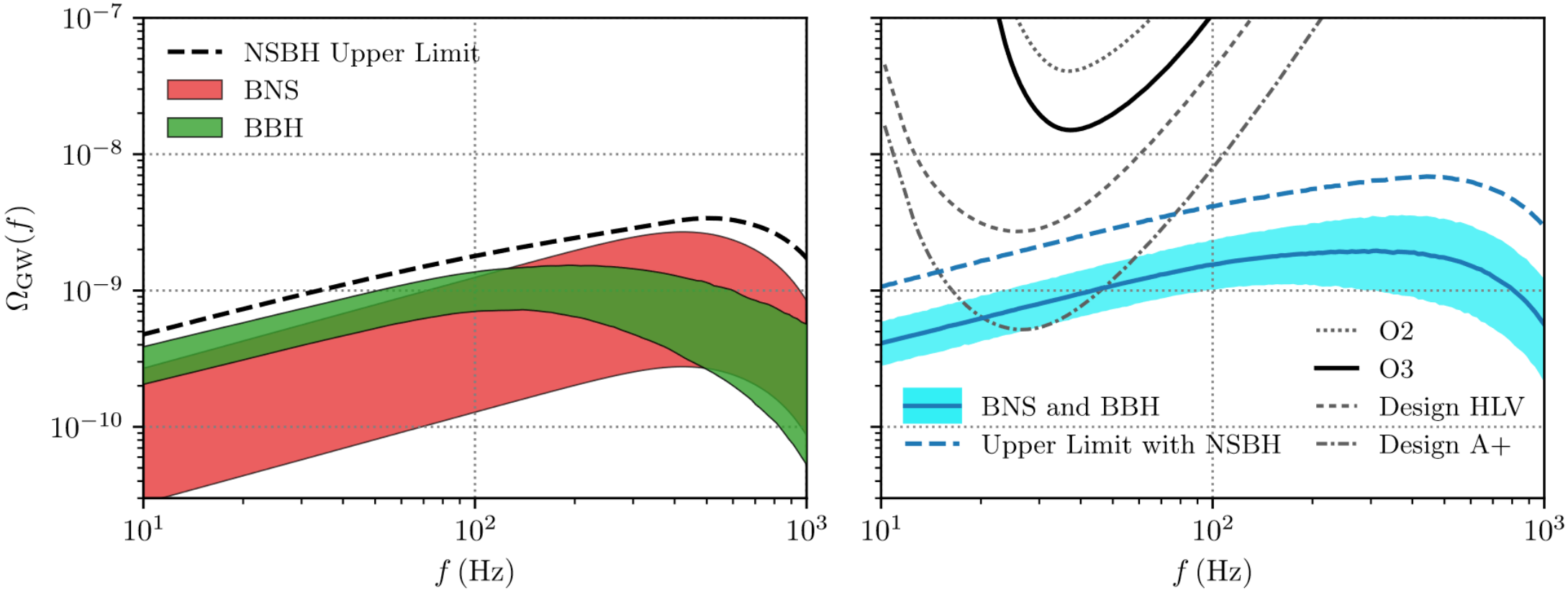

Fig. 8: The expected contribution of BBHs and BNS to the astrophysical background based on O1-O3 merger events. Shown together with the sensitivity curves for O2, O3 and future observing runs. Phys. Rev. D 104, 022004

Isotropic search for the SGWB

Optimal estimator is given by

$$\hat{C}^{IJ}(f) = \frac{2}{T} \frac{\mathrm{Re}[\tilde{s}_I^{\star}(f)\tilde{s}_J(f)]}{\gamma_{IJ}(f)S_0(f)}$$

Cross-correlation between detector I and J

Why?
SGWB signal is weak and similar to noise -> we need to combine detector signals to estimate.

BUT
Assumptions: uncorrelated noise, gaussian, stationary and isotropic.

Isotropic search for the SGWB

Optimal estimator is given by

$$\hat{C}^{IJ}(f) = \frac{2}{T}\frac{\mathrm{Re}[\tilde{s}_I^{\star}(f)\tilde{s}_J(f)]}{\gamma_{IJ}(f)S_0(f)}$$

Cross-correlation between detector I and J

Overlap reduction function for detector I and detector J: Accounting for differences of detectors in location and orientation.

$$S_0(f) = \frac{3H_0^2}{10\pi^2}\frac{1}{f^3}$$

Why?
SGWB signal is weak and similar to noise -> we need to combine detector signals to estimate.

BUT
Assumptions: uncorrelated noise, gaussian, stationary and isotropic.

We assume power-law form

$$\Omega_{\mathrm{GW}}(f) = \Omega_{\mathrm{ref}}\left(\frac{f}{f_{\mathrm{ref}}}\right)^{\alpha}$$

To get:

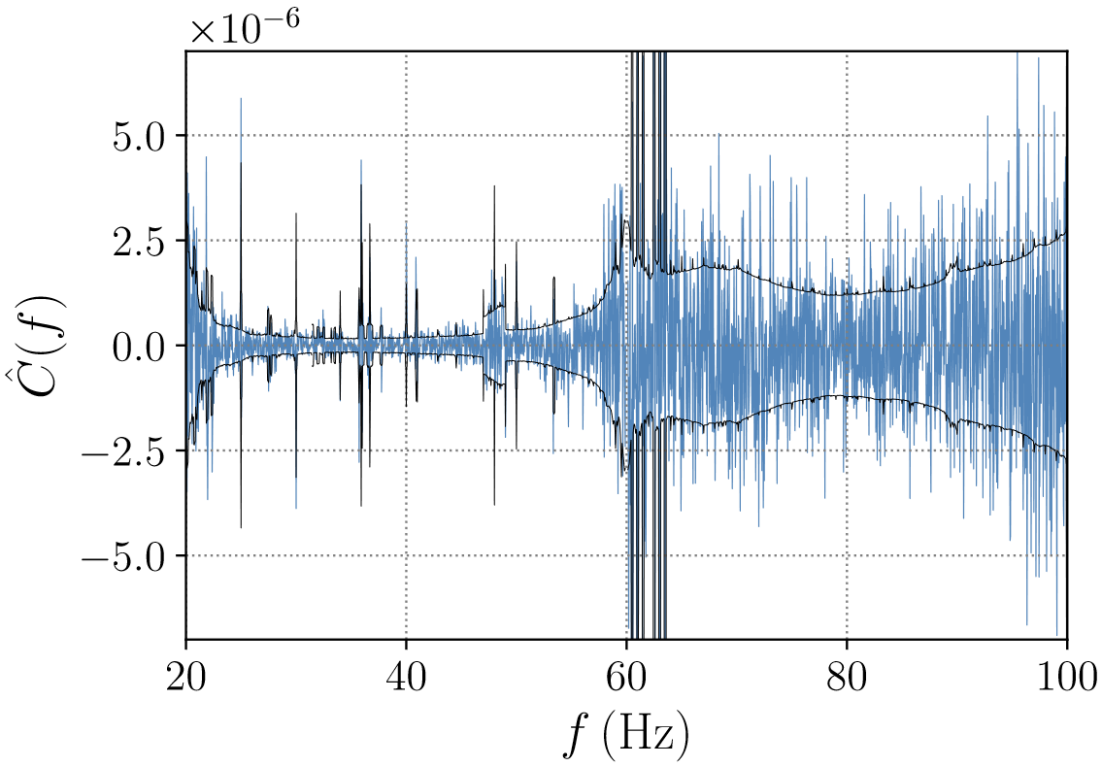

Fig. 9: Cross-correlation spectra in O3. LVK, Phys. Rev. D 104, 022004

Inferring the variation in redshift of the **binary black hole merger rate** combining gravitational-wave searches

Merger rate estimation

We split the merger rate $\mathcal{R}(z)$ of BBHs into three components:

$$\mathcal{R}(z) \sim p_{m_1} \cdot p_{m_2} \cdot p_z$$

Merger rate estimation

We split the merger rate $\mathcal{R}(z)$ of BBHs into three components:

$$\mathcal{R}(z) \sim p_{m_1} \cdot p_{m_2} \cdot p_z$$

Power-law plus peak

The most common model for the mass distribution of the heaviest black hole is the power-law plus peak model:

$$c_1 \cdot m_1^{-\kappa(z)} + c_2 \cdot e^{\frac{-(m_1-\mu_{m_1})^2}{2\sigma_{m_1}^2}}$$

Novelty: $p_{m_1}(\kappa_0) \rightarrow p_{m_1}(\kappa(z))$

$$\kappa(z) = \kappa_0 + z\mathrm{d}\kappa(z)/\mathrm{d}z$$

We add a redshift variation in the power-lax index of the distribution.

Merger rate estimation

We split the merger rate $\mathcal{R}(z)$ of BBHs into three components:

$$\mathcal{R}(z) \sim p_{m_1} \cdot p_{m_2} \cdot p_z$$

Power-law plus peak

The most common model for the mass distribution of the heaviest black hole is the power-law plus peak model:

$$c_1 \cdot m_1^{-\kappa(z)} + c_2 \cdot e^{\frac{-(m_1-\mu_{m_1})^2}{2\sigma_{m_1}^2}}$$

Novelty: $p_{m_1}(\kappa_0) \rightarrow p_{m_1}(\kappa(z))$

$$\kappa(z) = \kappa_0 + z\mathrm{d}\kappa(z)/\mathrm{d}z$$

We add a redshift variation in the power-lax index of the distribution.

The redshift distribution of the merger rate follows a **broken power-law**:

$$\mathcal{R}(z) \sim \frac{(1+z)^{\alpha}}{1+\left(\frac{1+z}{1+z_p}\right)^{\alpha+\beta}}$$

Merger rate estimation

We split the merger rate $\mathcal{R}(z)$ of BBHs into three components:

$$\mathcal{R}(z) \sim p_{m_1} \cdot p_{m_2} \cdot p_z$$

Power-law plus peak

The most common model for the mass distribution of the heaviest black hole is the power-law plus peak model:

$$c_1 \cdot m_1^{-\kappa(z)} + c_2 \cdot e^{\frac{-(m_1-\mu_{m_1})^2}{2\sigma_{m_1}^2}}$$

Novelty: $p_{m_1}(\kappa_0) \rightarrow p_{m_1}(\kappa(z))$

$$\kappa(z) = \kappa_0 + z\mathrm{d}\kappa(z)/\mathrm{d}z$$

We add a redshift variation in the power-lax index of the distribution.

Power-law

$m_1 > m_2$

The redshift distribution of the merger rate follows a **broken power-law**:

$$\mathcal{R}(z) \sim \frac{(1+z)^{\alpha}}{1+\left(\frac{1+z}{1+z_p}\right)^{\alpha+\beta}}$$

In previous studies, the joint chirps and stochastic background analysis never investigated the variation in redshift of mass distribution.

We add these two components together in a novel way.

Merger rate estimation

Power-law plus peak

$$p_{m_1}(\kappa_0) \rightarrow p_{m_1}(\kappa(z))$$

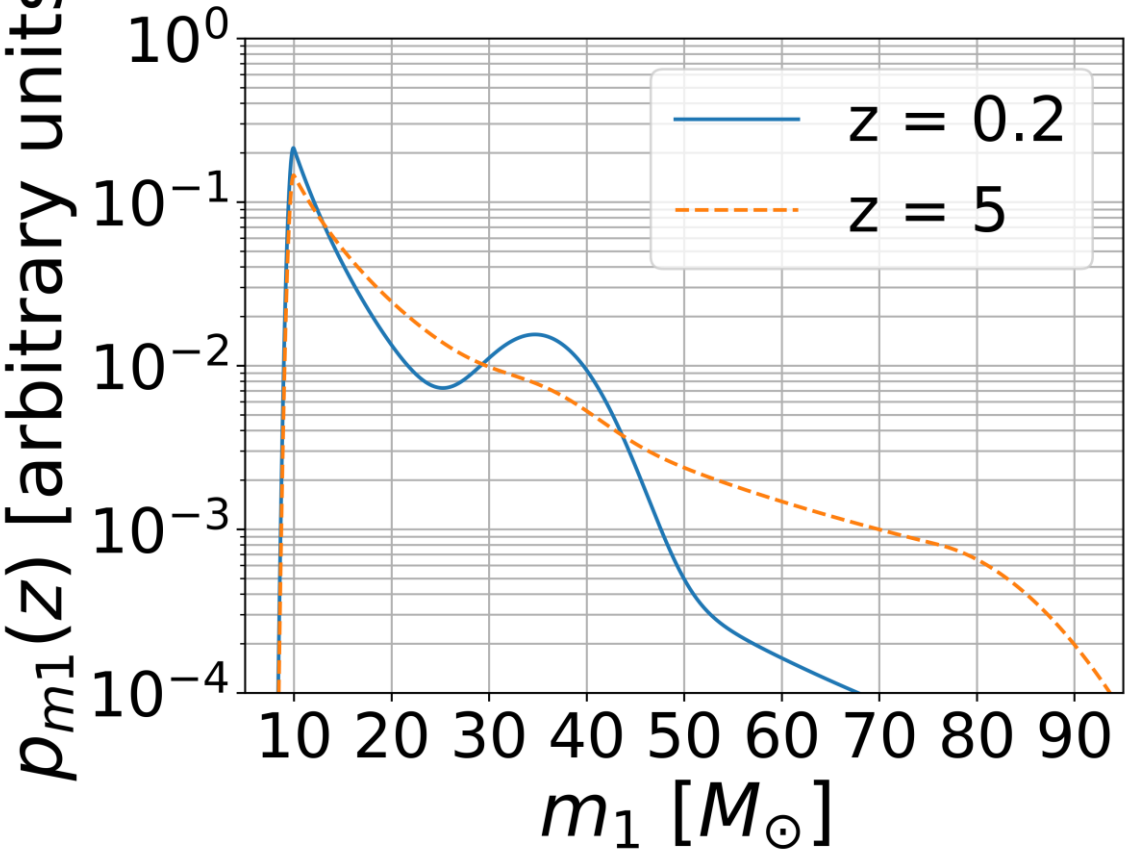

Fig. 10: Toy example of our novel power-law plus peak distribution.

Broken power-law

$$\mathcal{R}(z) \sim \frac{(1+z)^{\alpha}}{1+\left(\frac{1+z}{1+z_p}\right)^{\alpha+\beta}}$$

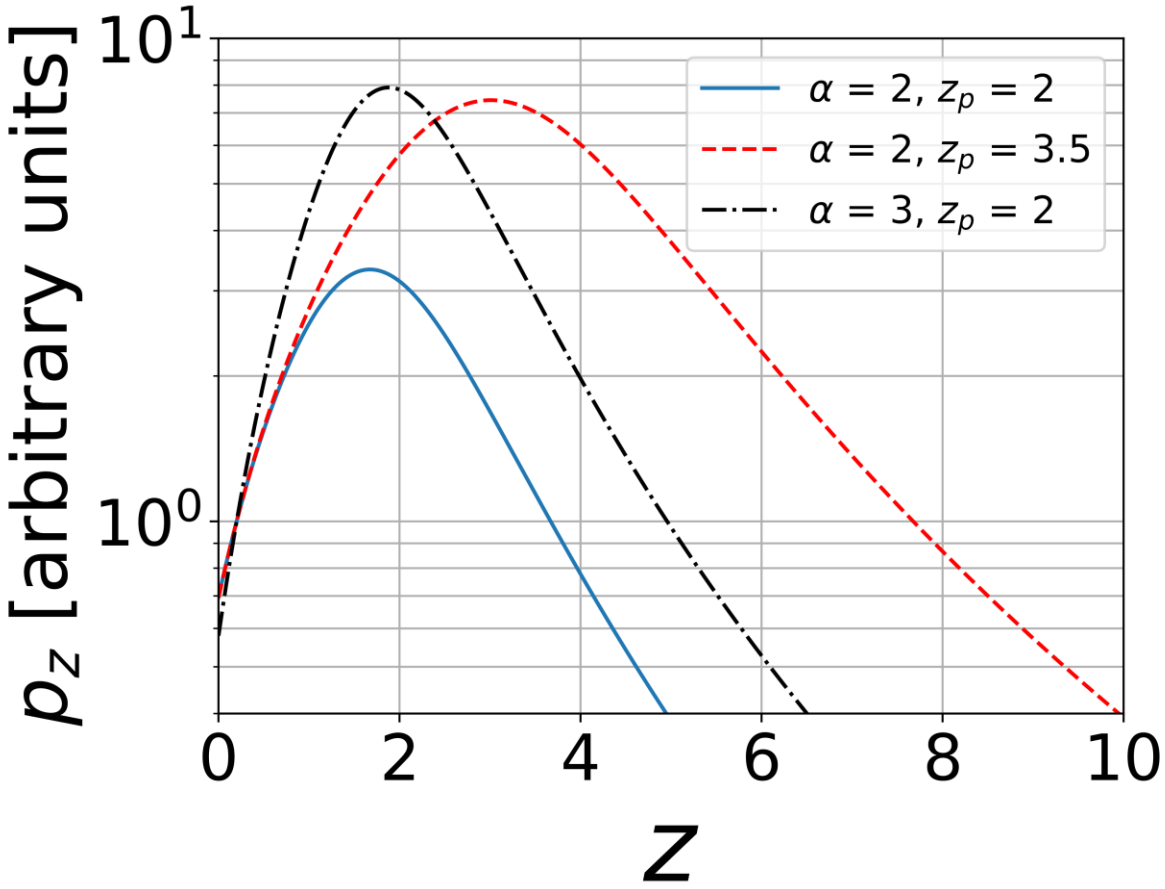

Fig. 11: Toy example of our broken power-law redshift distribution.

Inference

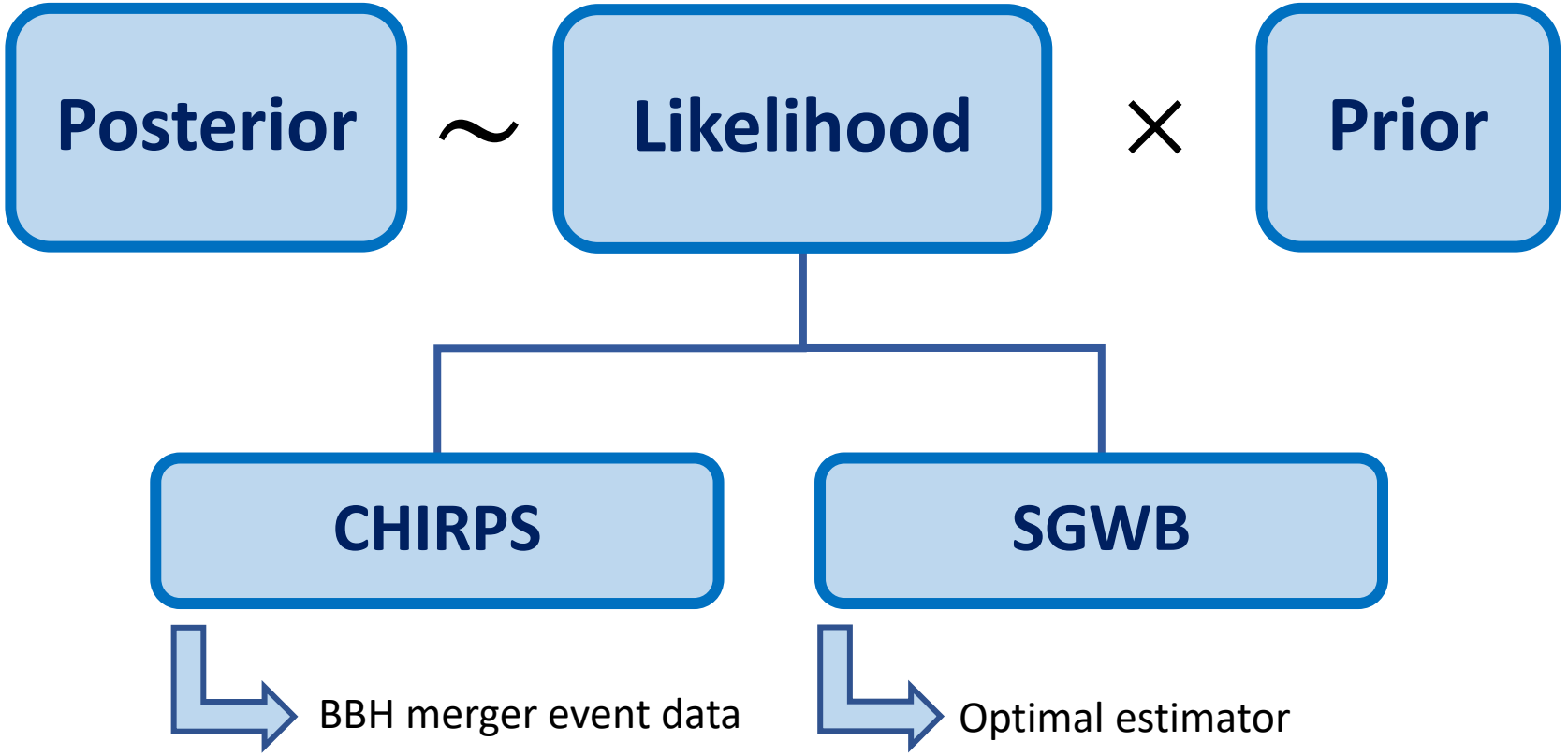

We are looking for the parameters representing the components of the merger rate:

- κ_0
- $d\kappa/dz$
- α
- z_p

Power-law plus peak model

Broken power-law model

O3 Results

BBH only analysis

BBH + GWB analysis

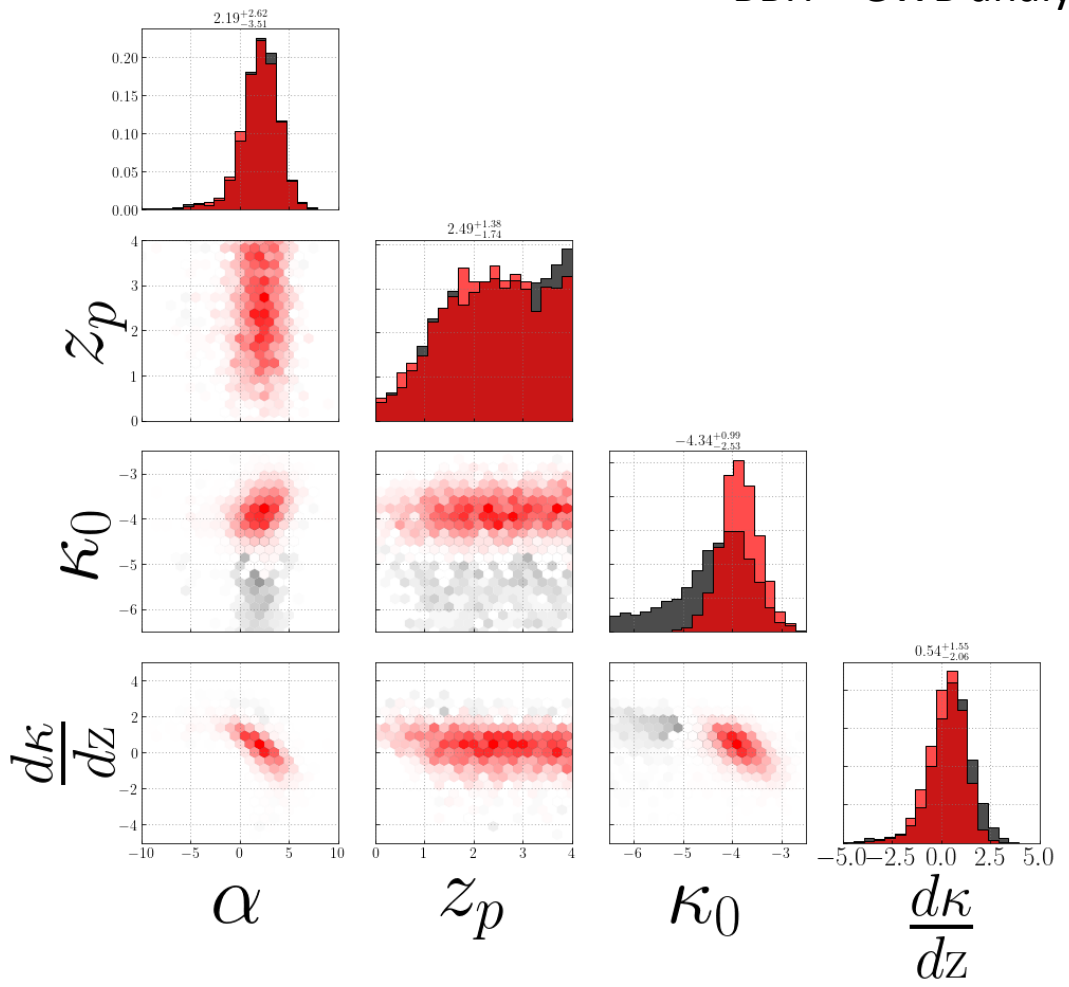

Fig. 12: Parameter Estimation (PE) results for O3 analysis, with and without GWB included.

Even without observing SGWB, we can learn about the merger rate and its variation in redshift.

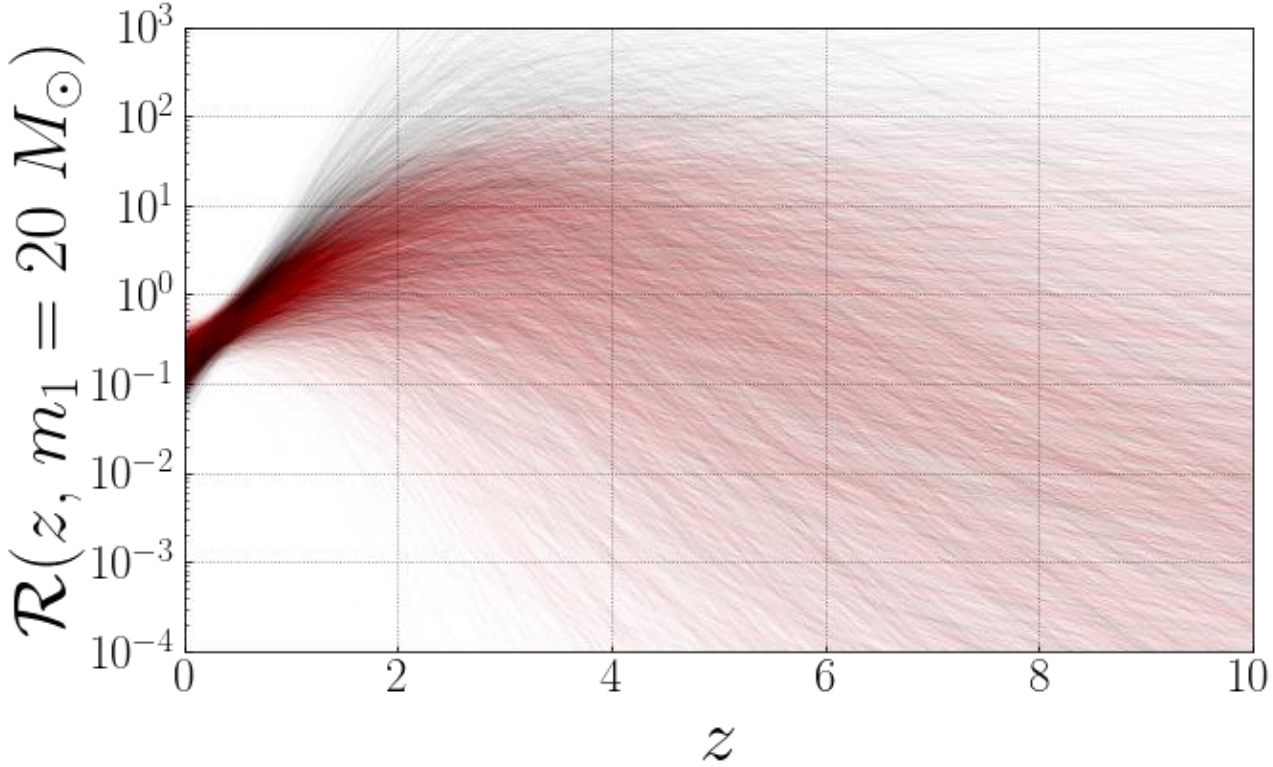

Fig. 13: The computed $\mathcal{R}(z)$ at fixed $m_1 = 20\ M_\odot$ for all samples of the O3 analysis. Once in red for the analysis where the GWB is included and once in black where only the direct BBH detections are considered.

Forecasting O5

We inject an O5-like GWB in data.
It is consistent with O3 BBH events.

Observing the SGWB adds information!
Peak redshift is different.

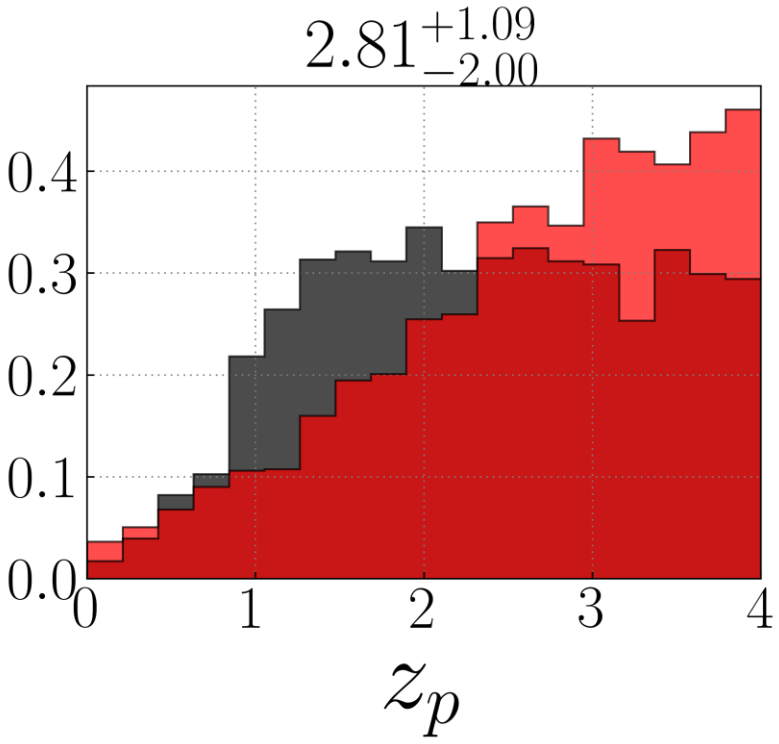

Fig. 14: PE results of the peak redshift for O5 considering a detected background. In red, we show the BBH+GWB analysis and in red, the BBH only analysis. The background detection adds information into the mix.

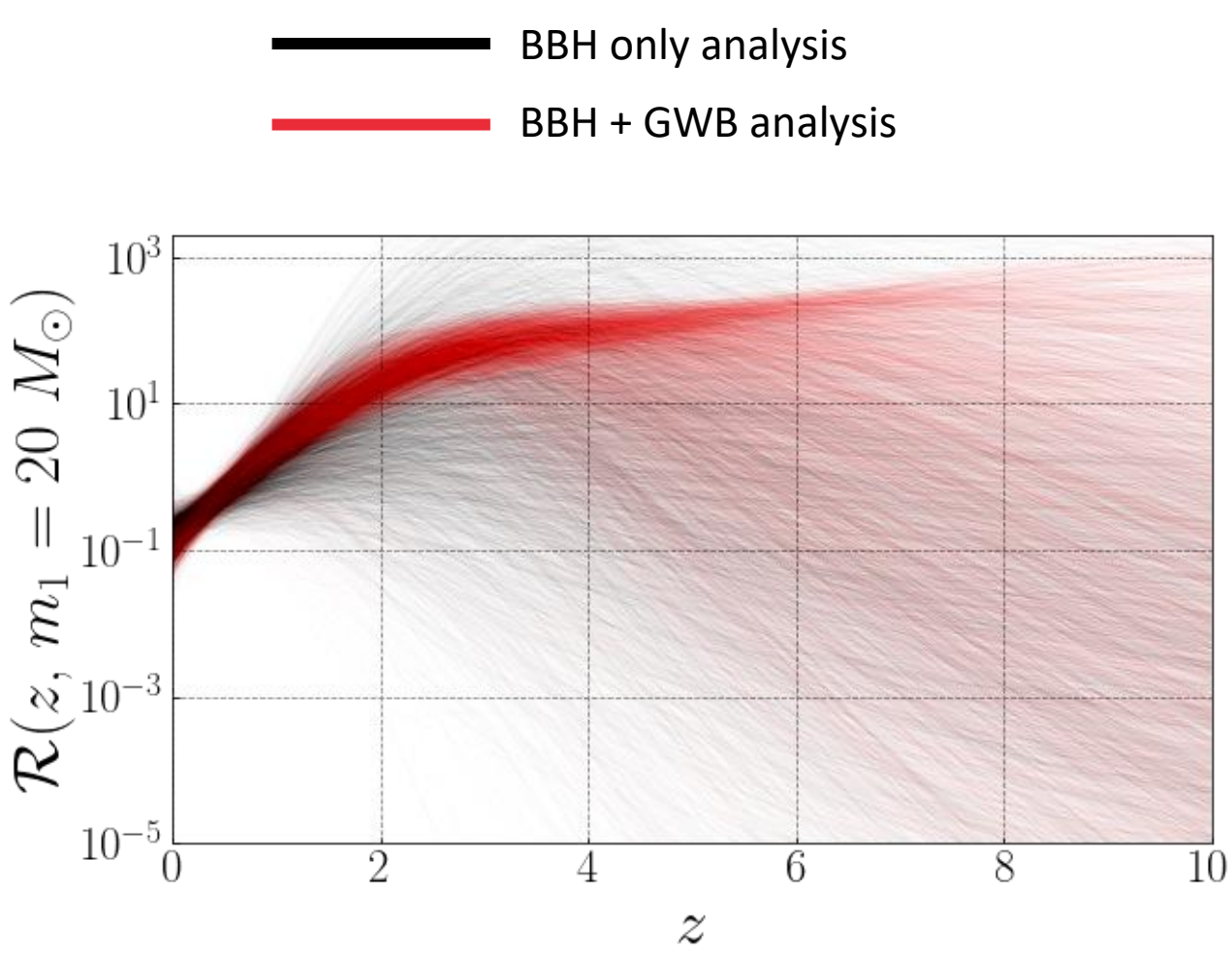

Fig. 15: The computed $\mathcal{R}(z)$ at fixed $m_1 = 20\ M_\odot$ for a detected background in O5. Once in red for the analysis where the GWB is included and once in black where only the direct BBH detections are considered.

O5 Results

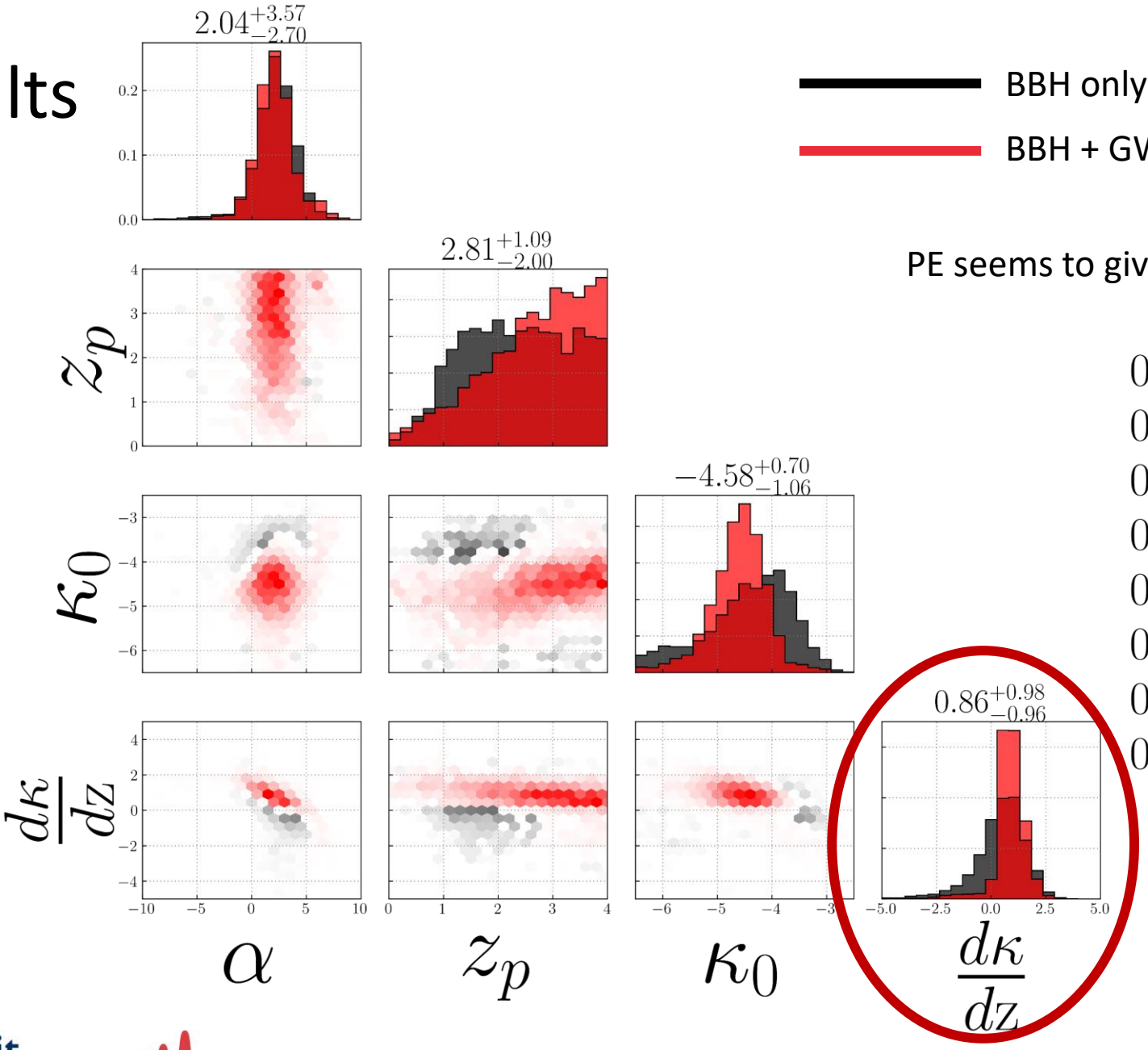

PE seems to give indication for variation in redshift.

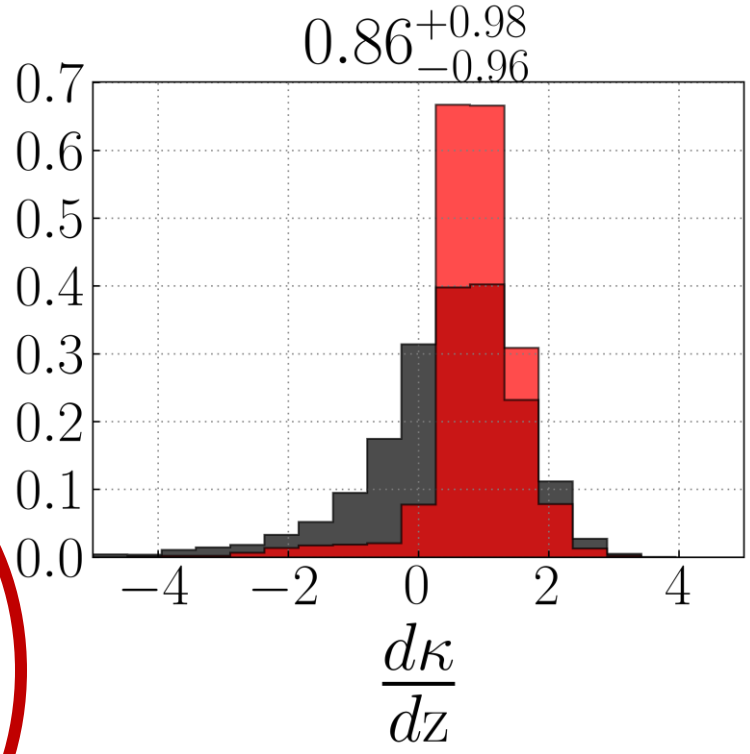

Fig. 16: PE results for O5 analysis using a detectable GWB, with and without GWB included in the analysis.

We highlight the posterior on the variation in the power-law of the power-law plus peak model, characterizing the variation in redshift.

Conclusion and outlook

Adding SGWB data improves knowledge on merger rate distribution.
We can constrain variation in redshift when considering mass distribution.
A possible detection of the SGWB gives improved constraints.
It can also give indication of the variation in redshift.

In future we can:

- **Vary different parameters**, investigating their evolution with redshift and how they might influence the merger rate evolution, e.g., varying peak redshift.
- **Investigate** the effect of variation with redshift on **possible formation channels** of BBHs.
- **Perform again in O4** after adding more chirps and improved stochastic upper limits.
- **Extend** the analysis to **binary neutron star** mergers.

Back-up slides

Forecasting O5

We compute the energy density of the background $\boldsymbol{\Omega_{GW}(f)}$ for all realized samples of O3.

$$\Omega(f) = \frac{f}{\rho_c} \int_0^{z_{\max}} dz \frac{\mathcal{R}(z) \left\langle \frac{dE_s}{df_s}|_{f(1+z)} \right\rangle}{(1+z)H(z)}$$

Each computed background is shown on Fig. A1 as a blue line.

One sample is taken and will serve as a toy model for the detected SGWB in O5.

We inject it our analysis and perform PE just as in O3 analysis.

The sensitivity curves of O3 and O5 [11] are represented by the red lines. One sample which can be detected in O5 is chosen and injected into our analysis.

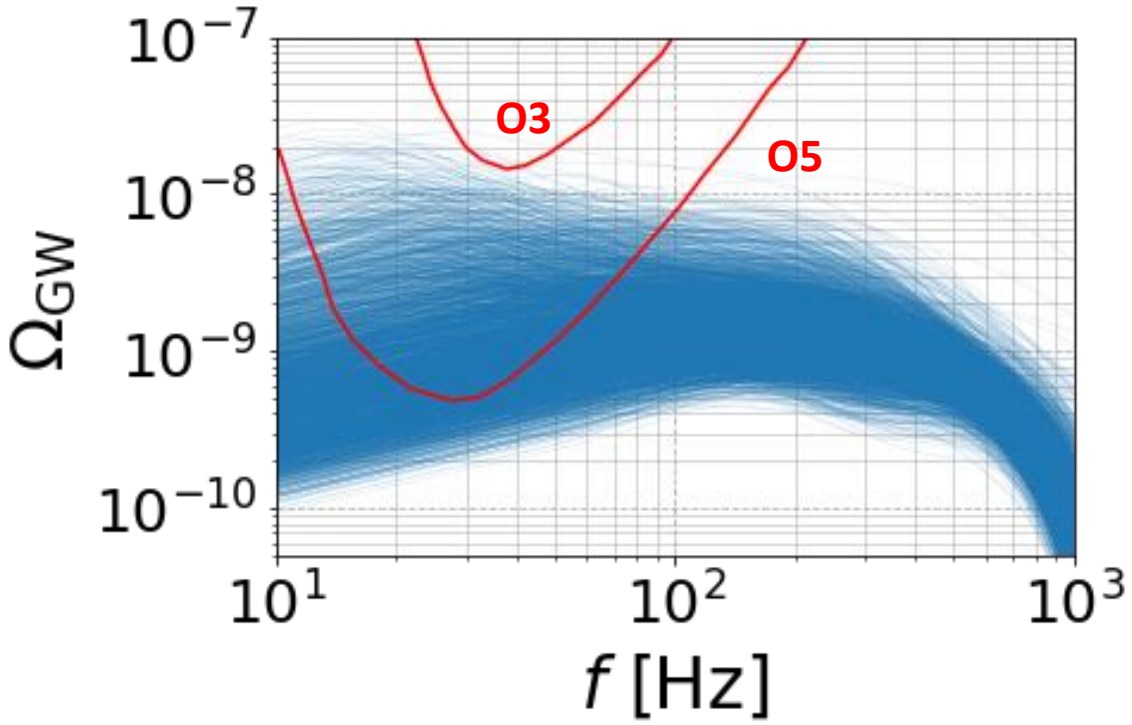

Fig. A1: The energy density of the background is computed for all samples in our analysis using the stochastic upper limits and direct BBH detections from O3.

More PE for O5

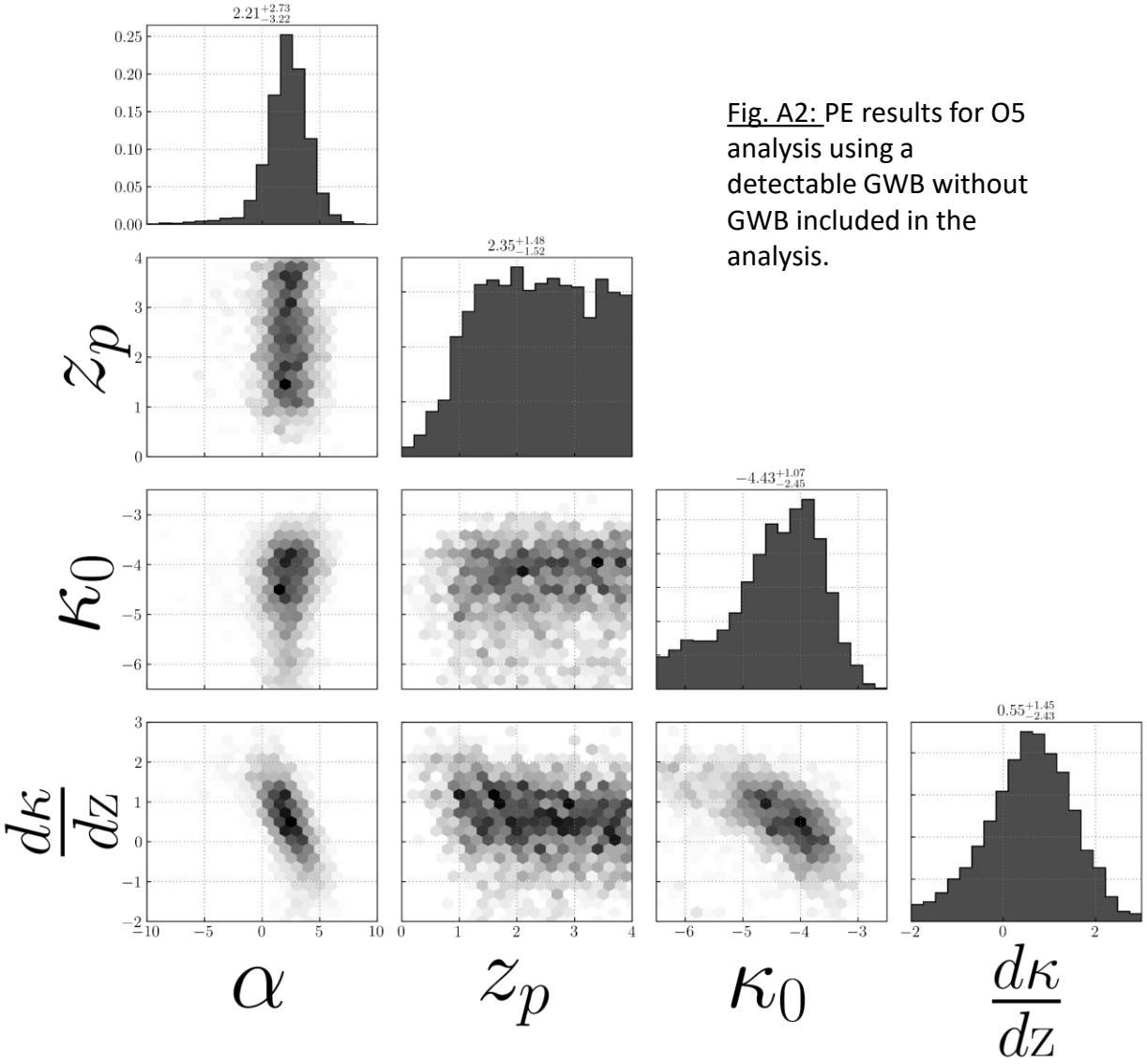

Fig. A2: PE results for O5 analysis using a detectable GWB without GWB included in the analysis.

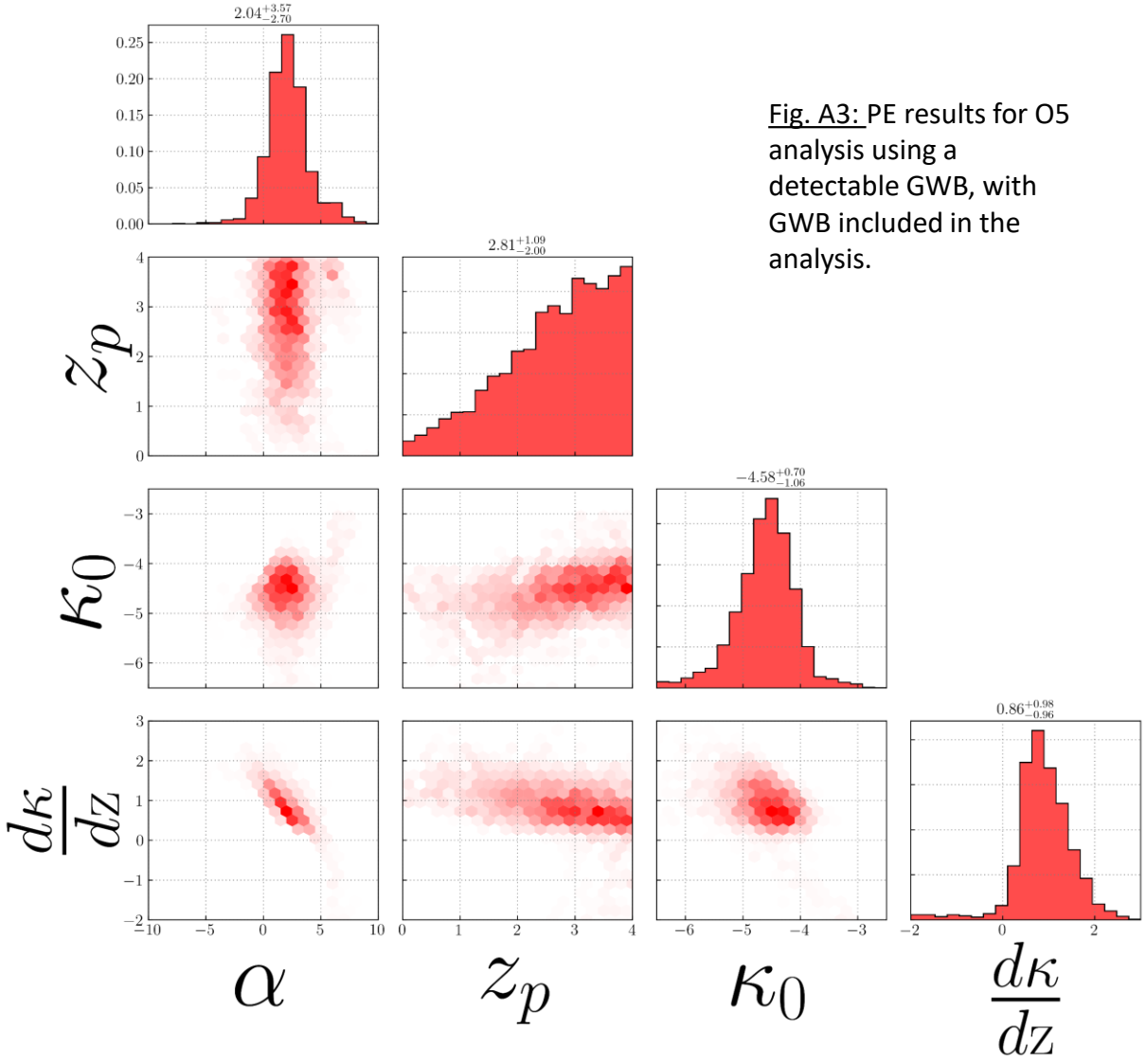

Fig. A3: PE results for O5 analysis using a detectable GWB, with GWB included in the analysis.

More PE for O5

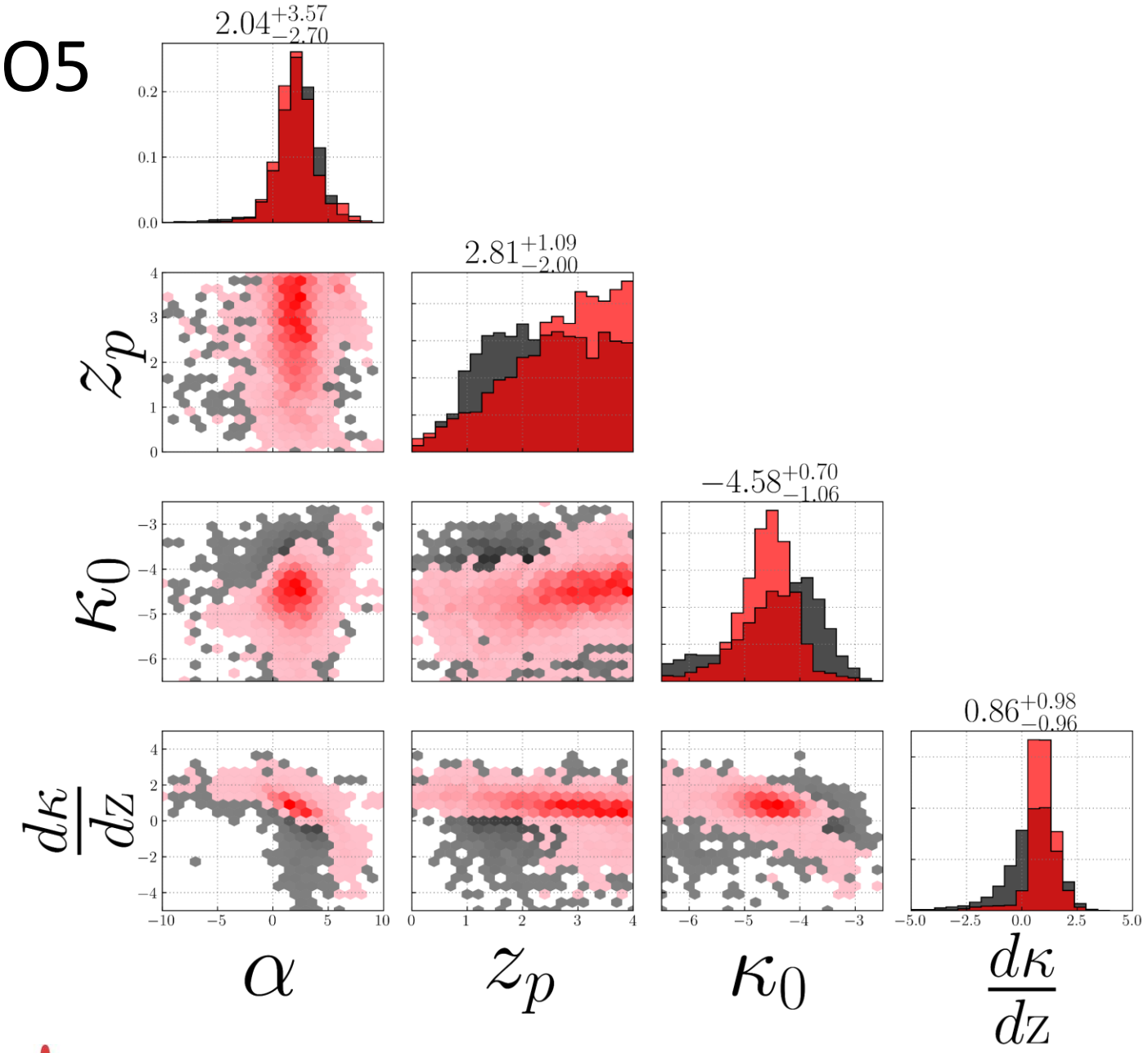

Fig. A4: PE results for O5 analysis using a detectable GWB, with and without GWB included in the analysis. Now with 2-D plots more clear.

Another way to look at it for O5

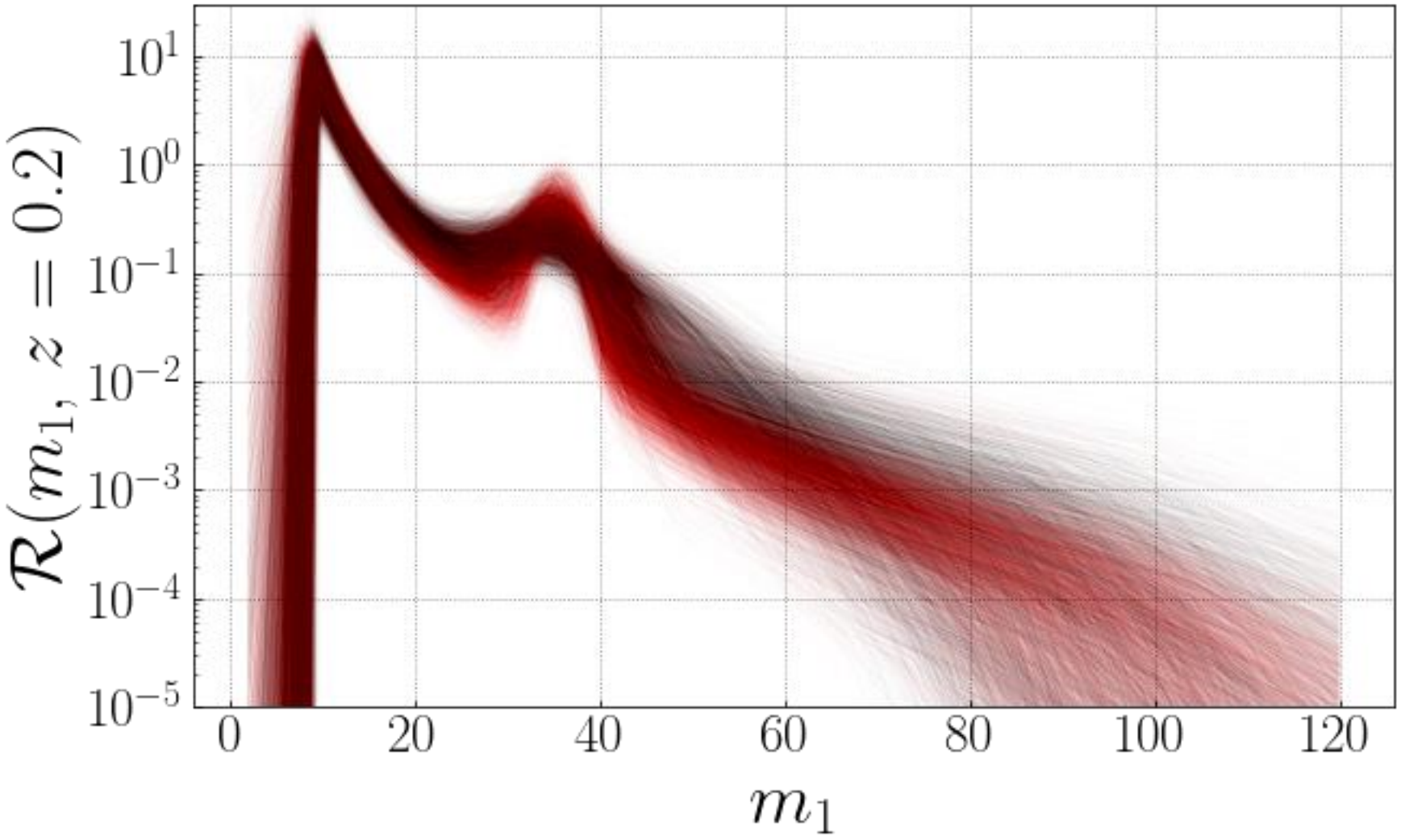

Fig. A5: Figure of $\mathcal{R}(m_1)$ at z = 0.2 for all samples in the O5 analysis. Once again, in red, we have the BBH+GWB analysis and in red the BBH only analysis.

We can observe a slight difference in the power-law index, even at these low redshifts.

More PE for O3

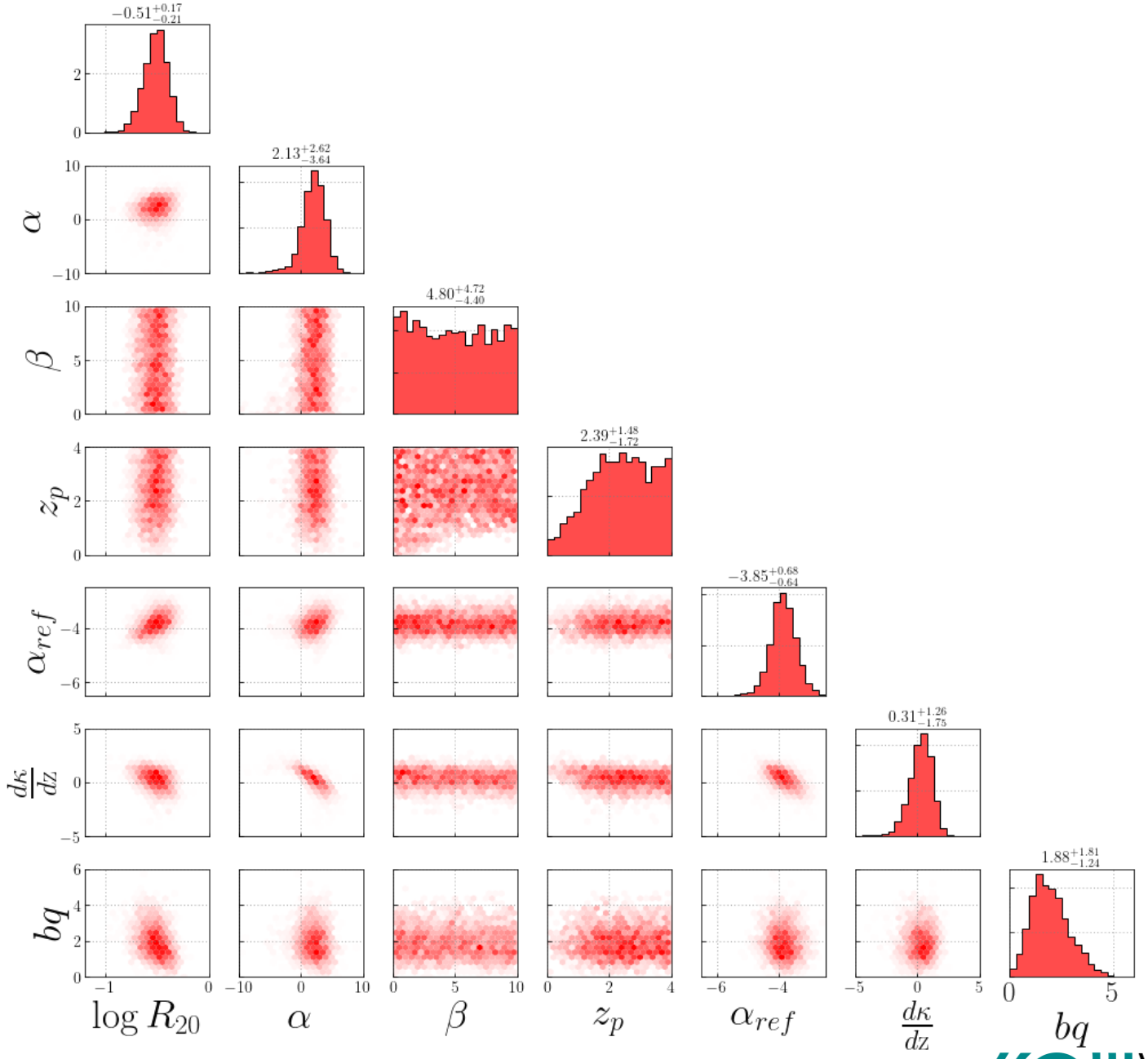

Fig. A6: PE results for O3 analysis (so no background observed), with GWB included in the analysis.

We also show all other possible hyperparameters here. Second index of broken power-law β gives back almost the prior.

Power-law integrated sensitivity curves

Idea from [Phys. Rev. D 88, 124032]

- Take network of detectors and compute effective energy density via effective strain power spectral density
- Assume an observation time T
- For set of power-law indices and a reference frequency, calculate value of amplitude such that SNR is equal to a fixed value

- For each pair of (index, amplitude), plot $\Omega_{GW}(f) = \Omega_\beta(\frac{f}{f_{ref}})^\beta$
- The envelope of these curves is the PLIS for two (or more) detectors, given by $\Omega_{PL}(f) = max_\beta[\Omega_\beta(f/f_{ref})\hat{}(\beta)]$

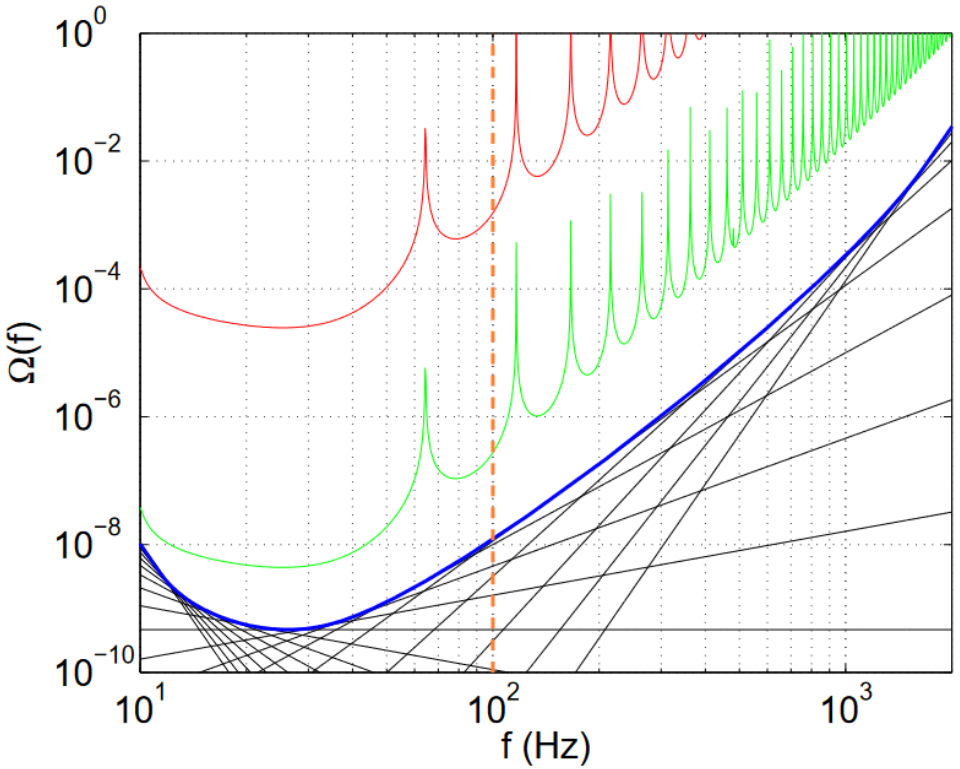

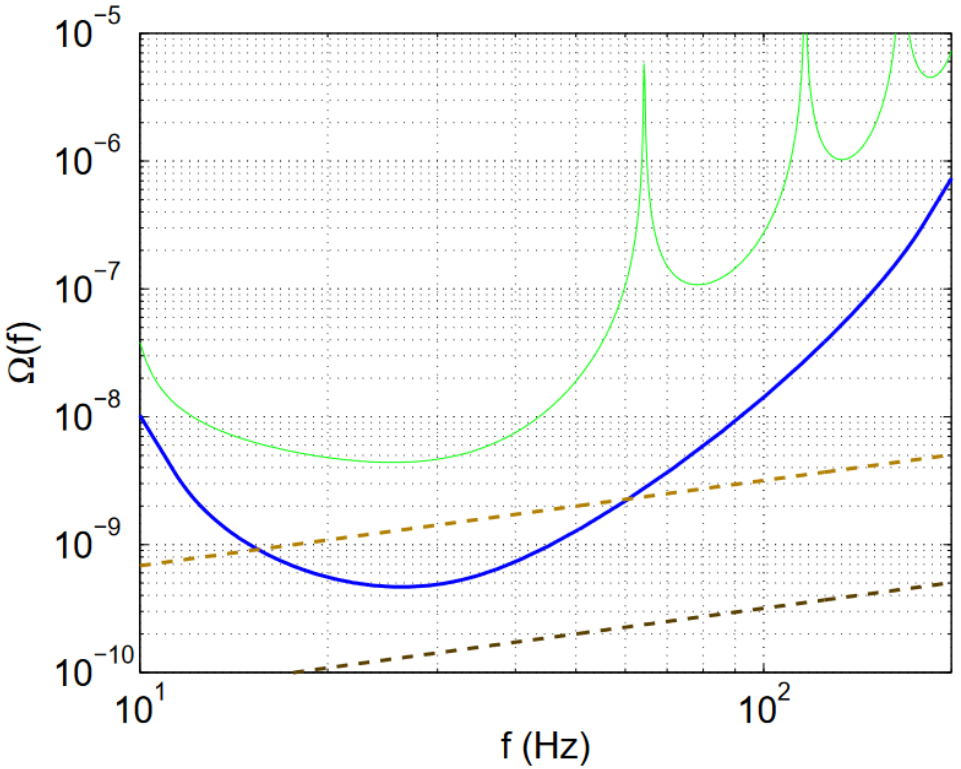

Fig. A7: The figure shows the making of the PLIS. On the left, one can see the black curves, which are the index, amplitude pairs plotted and in blue the computed PLIS. [Phys. Rev. D 88, 124032]

Overlap reduction function

$$\gamma(f) = \frac{5}{8\pi} \sum_A \int_{\text{Sky}} F_1^A(\hat{\boldsymbol{n}}) F_2^A(\hat{\boldsymbol{n}}) e^{2\pi i f \Delta \boldsymbol{x} \cdot \hat{\boldsymbol{n}}/c} d\hat{\boldsymbol{n}}.$$

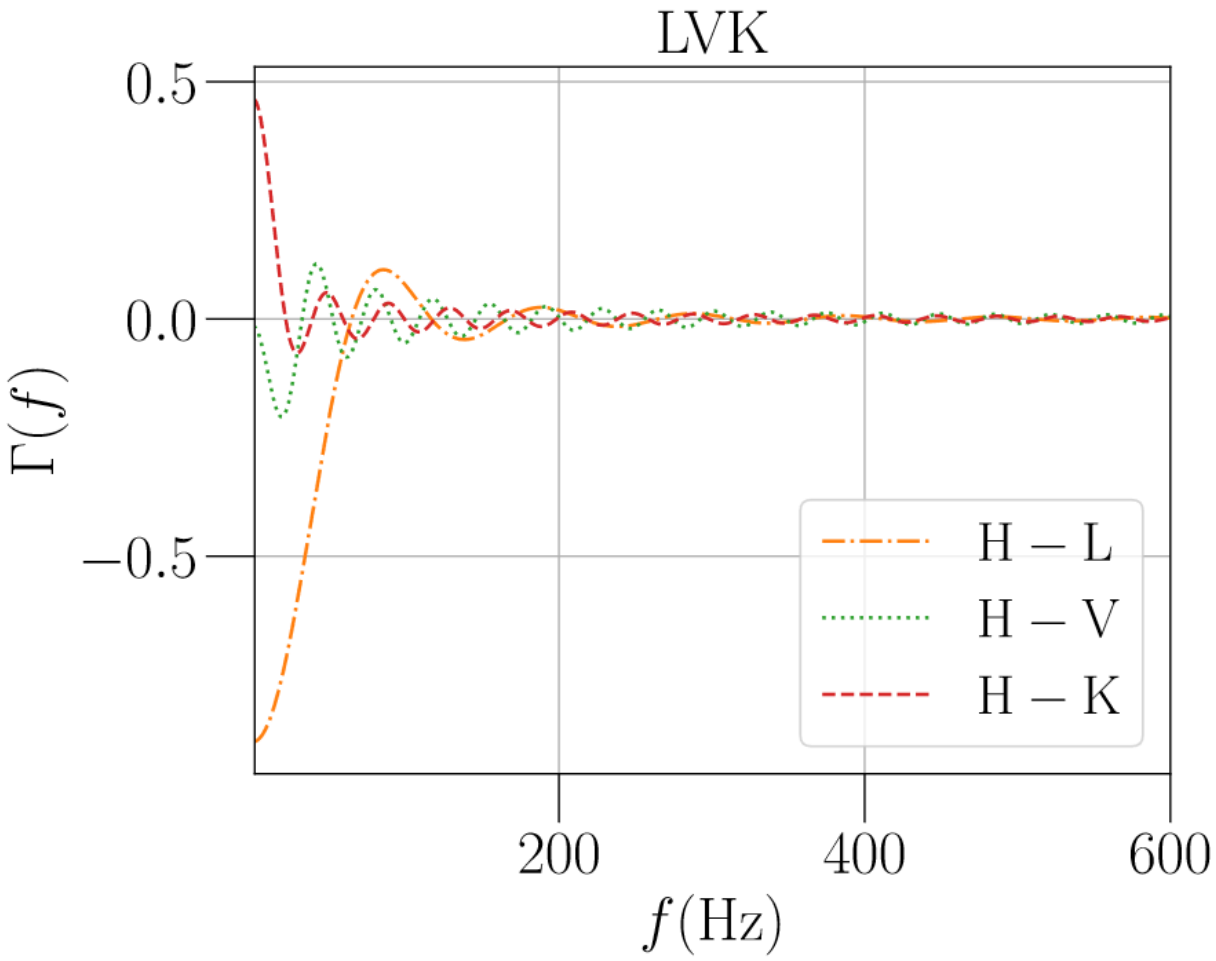

There is a tool exploiting this overlap reduction function for SGWB detection: **Geodesy:**
- T. A. Callister et al., 2018 ApJL 869 L28
- Janssens et al., Phys. Rev. D 105, 082001

Fig. A8: Graph showing all overlap reduction functions of the LVK network between H and the other detectors. It becomes quite small immediately for higher frequencies. Galaxies 2022, 10(1), 34.

Likelihood

We write down our likelihood as

$$p(\hat{C}, \{d_i\}|\Lambda, \mathcal{R}_0) = p_{\rm BBH}(\{d_i\}|\Lambda, \mathcal{R}_0) p_{\rm stoch}(\hat{C}|\Lambda, \mathcal{R}_0)$$

Optimal estimator

BBH merger event data

$$\left[N(\Lambda, \mathcal{R}_0)\,\xi(\Lambda)\right]^{N_{\rm obs}} e^{-N(\Lambda,\mathcal{R}_0)\xi(\Lambda)} \times \prod_{i=1}^{N_{\rm obs}} \frac{\int p(d_i|\phi)p(\phi|\Lambda)d\phi}{\xi(\Lambda)}$$

$$\exp\left[-\frac{1}{2}\left(\hat{C} - \gamma\,\Omega_M(\Lambda, \mathcal{R}_0)|\hat{C} - \gamma\,\Omega_M(\Lambda, \mathcal{R}_0)\right)\right]$$

We are interested in the parameters Λ representing the components of the merger rate:

- κ
- $d\kappa/dz$

Power-law plus peak model

- α
- z_p

Broken power-law model

- $\mathcal{R}_0$: reference merger rate

The stochastic gravitational-wave background

Fig. A9: Overview of potential background signals across the frequency spectrum. Showing both sensitivity curves from experiments as dotted lines and expected background magnitudes as solid lines.
Galaxies 2022, 10(1), 34

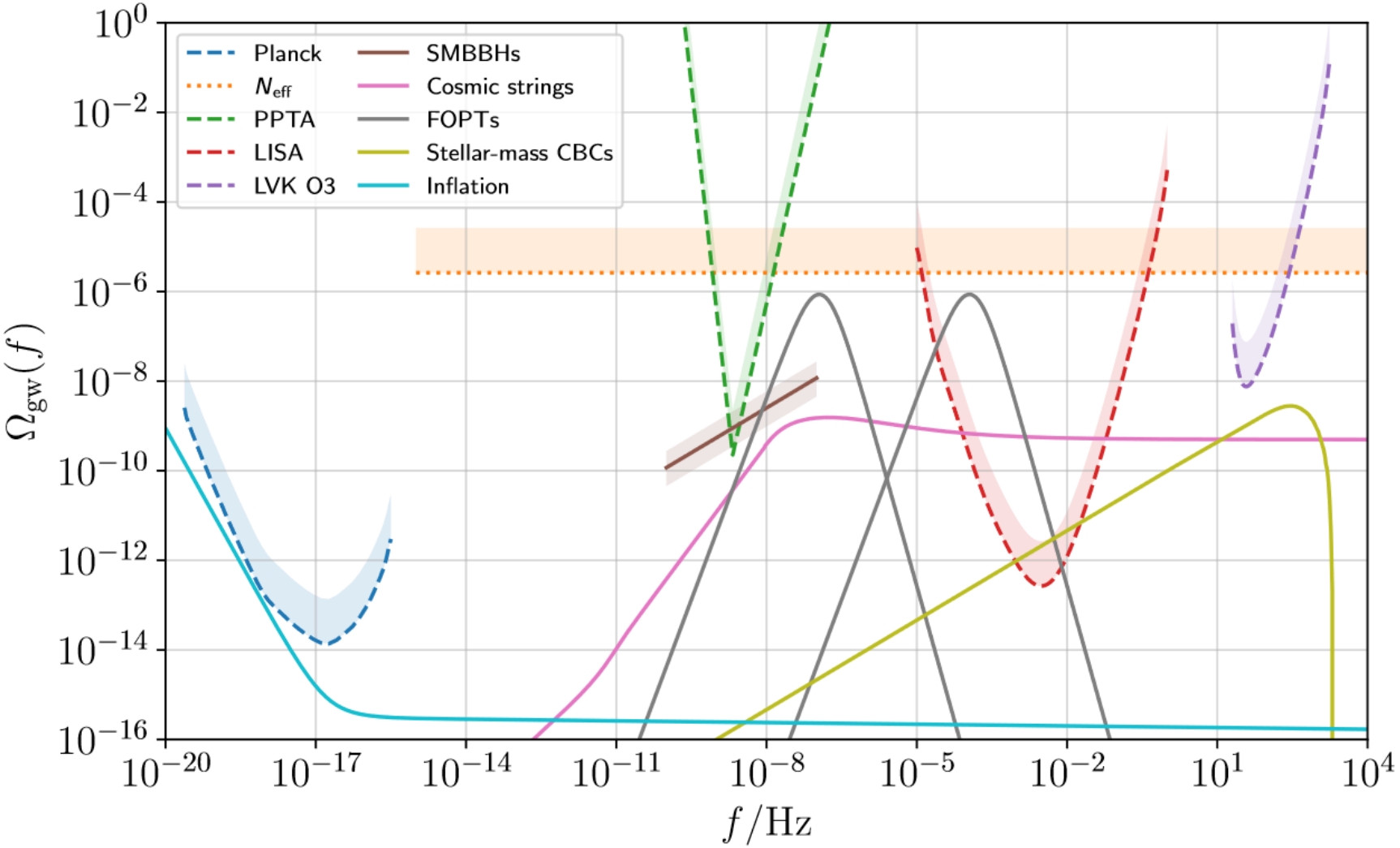

The stochastic gravitational-wave background: PTAs

LVK

PTAs

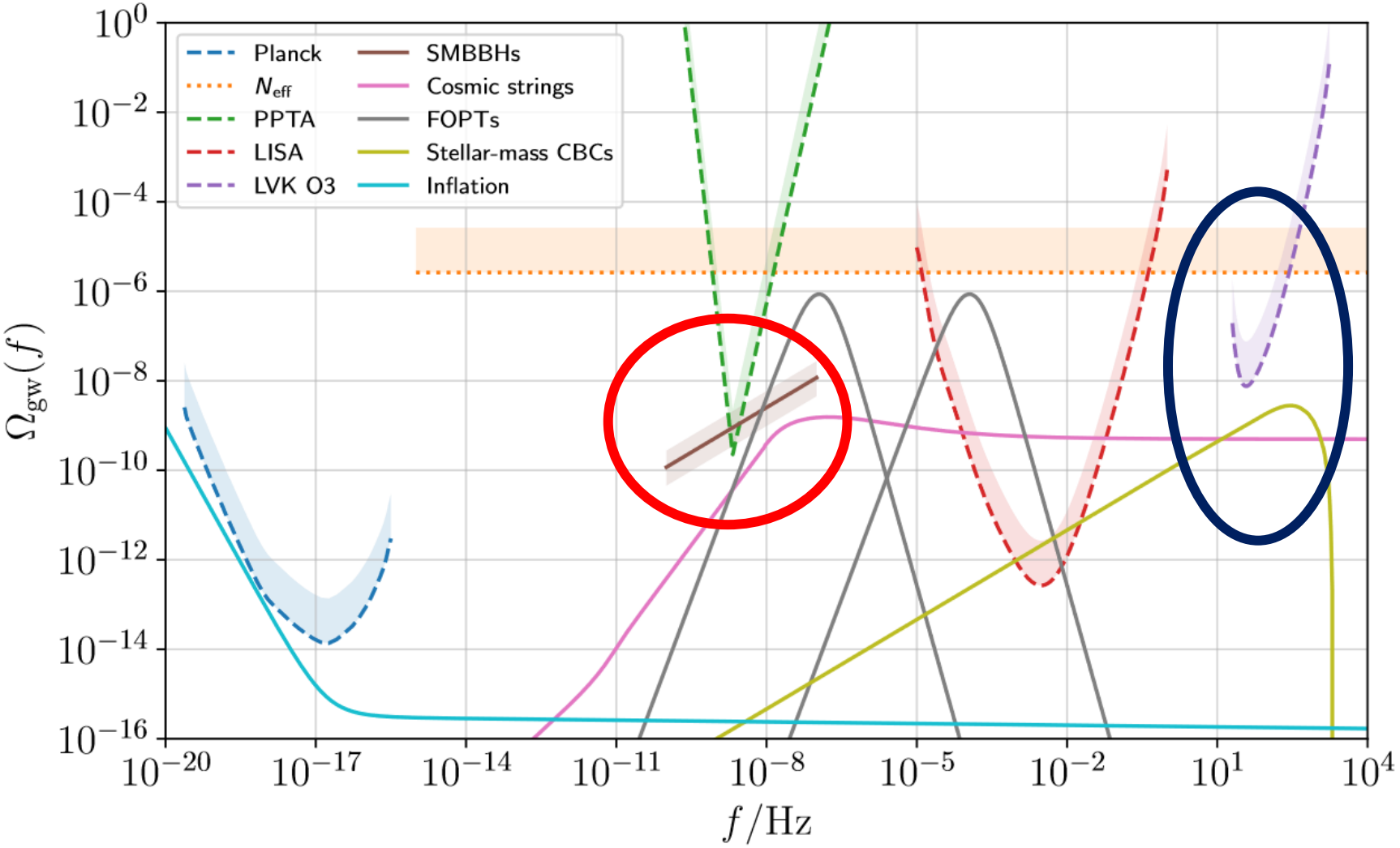

Fig. A10: Overview of potential background signals across the frequency spectrum. Showing both sensitivity curves from experiments as dotted lines and expected background magnitudes as solid lines.
Galaxies 2022, 10(1), 34

References

[1] B. P. Abbott et al., LIGO and Virgo Collaboration, Observation of Gravitational Waves from a Binary Black Hole Merger, Phys. Rev. Lett. 116, 061102

[2] R. Abbott et al., LIGO, Virgo, and KAGRA Collaboration, Population of Merging Compact Binaries Inferred Using Gravitational Waves through GWTC-3, Phys. Rev. X 13, 011048

[3] https://www.ligo.caltech.edu/LA/image/ligo20211107a

[4] R. Abbott et al., LIGO, Virgo, and KAGRA Collaboration, Upper limits on the isotropic gravitational-wave background from Advanced LIGO and Advanced Virgo's third observing run, Phys. Rev. D 104, 022004

[5] A. Renzini et al., Stochastic Gravitational-Wave Backgrounds: Current Detection Efforts and Future Prospects (2022), Galaxies 2022, 10(1), 34; https://doi.org/10.3390/galaxies10010034

[6] Arianna I. Renzini et al., pygwb: A Python-based Library for Gravitational-wave Background Searches (2023), *ApJ* **952** 25

[7] R. Abbott et al., LIGO, Virgo, and KAGRA Collaboration, GWTC-3: Compact Binary Coalescences Observed by LIGO and Virgo During the Second Part of the Third Observing Run. (2021). https://arxiv.org/abs/2111.03606

[8] Tom Callister et al., Shouts and Murmurs: Combining Individual Gravitational-wave Sources with the Stochastic Background to Measure the History of Binary Black Hole Mergers (2020), *ApJL* **896** L32

[9] https://www.virgo-gw.eu/science/detector/optical-layout/

[10] https://www.ligo.caltech.edu/image/ligo20160211c

[11] B.P. Abbott et al., LIGO, Virgo, and KAGRA Collaboration, Prospects for observing and localizing gravitational-wave transients with Advanced LIGO, Advanced Virgo and KAGRA. Living Rev Relativ 23, 3 (2020).

[12] Eric Thrane and Joseph D. Romano, Sensitivity curves for searches for gravitational-wave backgrounds, Phys. Rev. D 88, 124032